A NEW EMPIRICAL MODEL FOR THE PEAK IONOSPHERIC ELECTRON DENSITY USING NEURAL NETWORKS

THESIS

Submitted in fulfilment of the

requirements for the Degree of

MASTER OF SCIENCE

of Rhodes University

by

Lee-Anne McKinnell (née Williscroft)

December 1996

Abstract

This thesis describes the search for a temporal model for predicting the peak ionospheric electron density-(foF2). Existing models, such as the International Reference Ionosphere (IRI) and SKYCOM, were used to predict the 12 noon foF2 value over Grahamstown (26°E, 33°S). An attempt was then made to find a model that would improve upon these results. The traditional method of linear regression was used as a first step towards a new model. It was found that this would involve a multivariable regression that is reliant on guessing the optimum variables to be used in the final equation. An extremely complicated modelling equation involving many terms would result. Neural networks (NNs) are introduced as a new technique for predicting foF2. They are also applied, for the first time, to the problem of determining the best predictors of foF2. This quantity depends upon day number, level of solar activity and level of magnetic activity. The optimum averaging lengths of the solar activity index and the magnetic activity index were determined by appling NNs, using the criterion that the best indices are those that give the lowest rms error between the measured and predicted foF2. The optimum index for solar activity was found to be a 2-month running mean value of the daily sunspot number and for magnetic activity a 2-day averaged A index was found to be optimum. In addition, it was found that the response of foF2 to magnetic activity changes is highly non-linear and seasonally dependent. Using these indices as inputs, the NN trained successfully to predict foF2 with an rms error of 0.946 MHz on the daily testing values. Comparison with the IRI showed an improvement of 40% on the rms error. It is also shown that the NN will predict the noon value of foF2 to the same level of accuracy for unseen data of the same type.

DECLARATION

I, Lee-Anne McKinnell, declare the contents of this thesis to be the product of my own work.

This thesis has been partially presented by myself and co-authored by Dr Allon Poole at the following local conferences:

- South African Institute of Physics 1995
- Antennas and Propogation & Microwave Theory and Techniques Symposium 1995
- South African Institute of Physics 1996

The contents of chapter 6 formed a paper which was presented at the International Union of Radio Science (URSI) General Assembly held in Lille, France in August 1996.

The contents of chapter 5 and chapter 6 are the subject of a paper which was accepted for publication in Geophysical Research Letters on 31 October 1996.

This thesis is being submitted for the degree of Master of Science in Physics at Rhodes University, Grahamstown. It has not been submitted for any degree or examination at any other University.

Lee-Anne McKinnell (née Williscroft)

Student No. 689W5120

ACKNOWLEDGEMENTS

Firstly, I would like to take this opportunity to thank my supervisor, Dr Allon Poole, for making this project possible. His continued support and encouragement were invaluable to me.

I would like to express my appreciation to Grinaker Systems Technologies (GST) for their financial support. In particular, for making my attendance at the International Union of Radio Science (URSI) General Assembly in Lille, France, possible.

The magnetic data used for the research presented in this thesis was obtained from the Hermanus Magnetic Observatory. I thank them, in particular Louis Loubser, for their generous help.

To my husband, John, thank you for showing me that I don't have to walk alone.

Contents

List of Figures

List of Tables

Chapter 1

INTRODUCTION

The ionosphere is that region of the upper atmosphere that lies between 50km and 600km above the earth's surface. Extreme Ultraviolet light (EUV) from the sun is the main cause of the ionization that takes place between these altitudes. *McNamara [1991]* gives a detailed description of the processes at work in the ionosphere.

The ionosphere is useful to a variety of people including high frequency communicators and ionospheric or plasma physicists. High frequency radio signals can be received and transmitted from anywhere in the world via the ionosphere and it is therefore seen as a useful propagation medium.

At any one time the ionosphere may contain up to four different layers at different altitudes. During the day, the layers are : the D layer (50km to 100km), the E layer (100km to 200km), the F1 layer (200km to 300km) and the F2 layer (above 300km). At night, only a diminished F2 layer is present due to the absence of the influence of the sun on the ionosphere.

The behaviour of the ionosphere depends on a variety of geophysical and solar-terrestrial parameters. These parameters include geographical position, time of day, season, solar cycle and level of geomagnetic activity. As a result of this, the ionosphere is an extremely variable medium.

An ionospheric sounder, called an ionosonde, is used to monitor the behaviour of the ionosphere. High frequency radio waves are propagated into the ionosphere and the delay time between transmitting and receiving the signal is measured. The ionosonde outputs a plot of virtual height versus frequency, which is called an ionogram. This ionogram is a graphical representation of the ionospheric state. An electron density profile illustrates the way in which the electron density varies with height and can be obtained from the ionogram. An ionogram and electron density profile for a typical daytime condition is shown in figure 1-1.

The longest global time series of data is provided by vertical incidence ionosonde measurements. These ionosondes are therefore the most important worldwide data source for predicting ionospheric characteristics. A vertical incidence ionosonde has been operating in Grahamstown (26°E,33°S) for over 20 years and ionospheric data from two solar cycles has been collected and archived. Grahamstown is therefore a good base for ionospheric research.

Several important ionospheric characteristics can be obtained from the ionogram and corresponding electron density profile. These include the critical frequencies of each layer, the minimum frequency, the maximum useable frequency (MUF), and the heights at which these frequencies occur. The critical frequency of a layer is the maximum frequency which can be reflected from it at vertical incidence. The electron density, N_mF, at the height where reflection occurs is related to the critical frequency, f, by the relationship

$$N_mF/m^{-3} = 1.24 * 10^{10}(f/MHz)^2$$

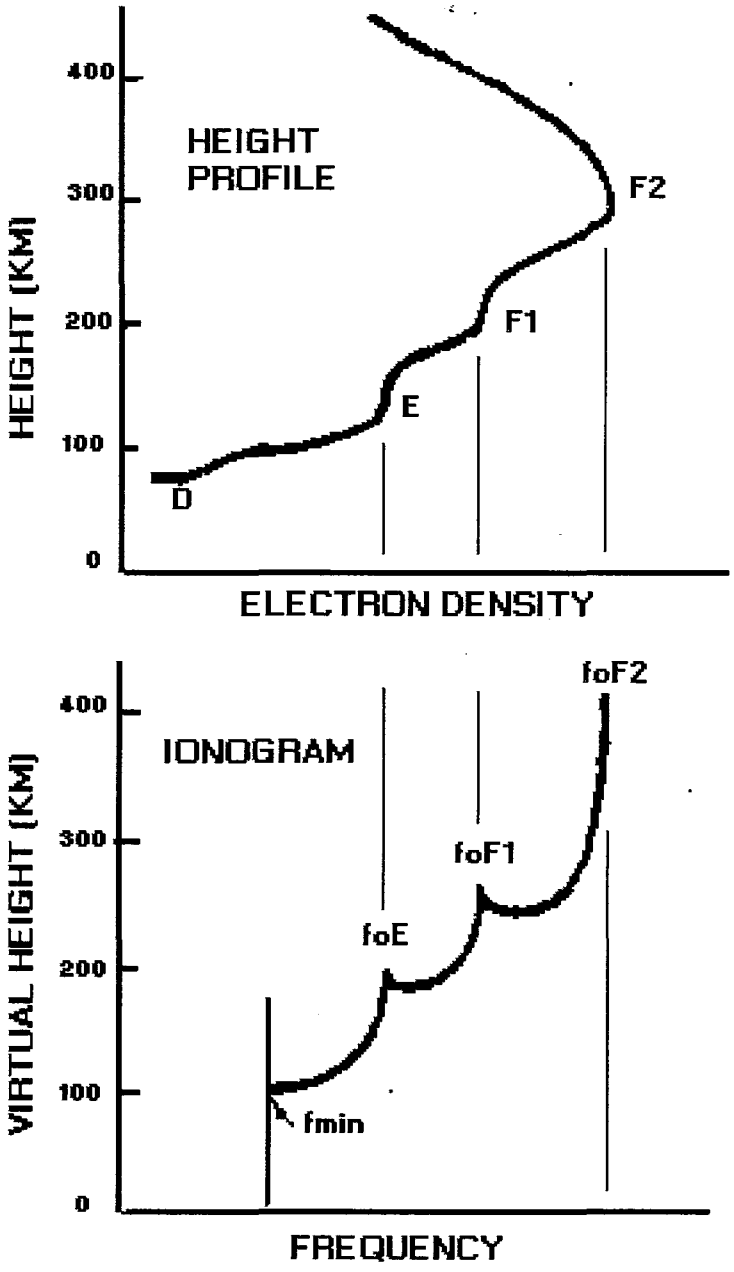

Figure 1-1: A typical daytime ionogram and corresponding electron density profile is shown. The critical frequencies and electron densities for each layer are indicated. *After McNamara [1991].*

Each layer has a critical frequency assigned to it, denoted by foE, foF1 and foF2. The F2 layer is important for long-distance communications and is the most variable layer. This layer is present all the time. foF2 is the critical frequency of the F2 layer and the frequency at which maximum electron density of the ionosphere occurs. Figure 1-1 indicates foF2 and its corresponding electron density for a typical daytime situation. The critical frequencies and maximum electron densities of the other layers are also shown.

The traditional user of the ionosphere is the high frequency (HF) communicator. Even though the ionosphere is a natural source and therefore sometimes uncooperative, it does have advantages over more modern carriers of communication such as satellites. For example, some countries may not be able to afford to install satellite links and therefore will have to rely on a cheaper medium.

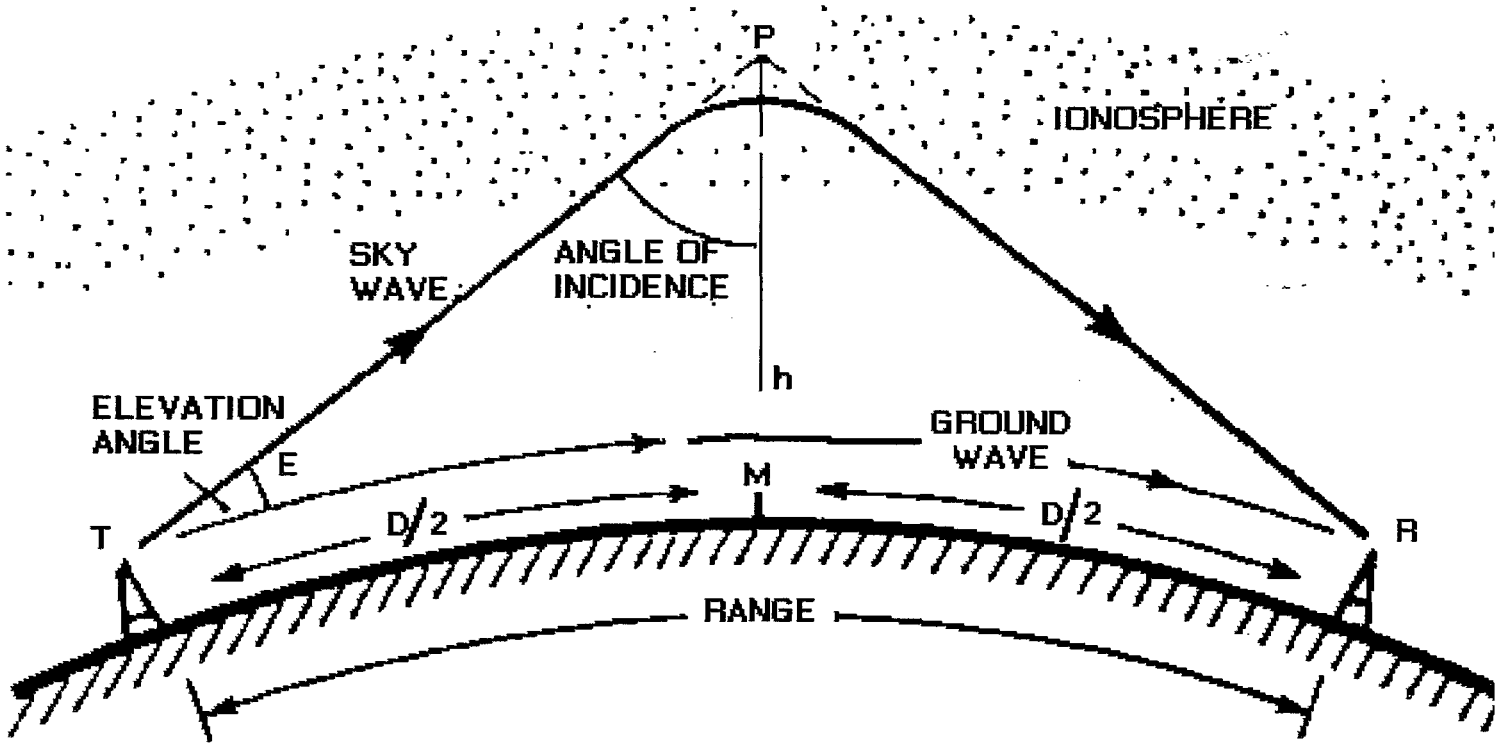

Figure 1-2: This diagram shows the path taken by a radio wave travelling between a transmitter (T) and a receiver (R). The skywave is reflected from the ionosphere at a point P down towards the receiver. *After McNamara [1991].*

Single Site Location (SSL) is a technique which relies on signals being reflected from the ionosphere. SSL is a direction finding system for determining the location of a transmitter by measuring the elevation angle of the incoming radio waves as well as their azimuth. By tracing the radio waves back from the SSL site to the transmitter the location of the transmitter can be determined. This setup is detailed in figure 1-2. Practical applications of the SSL technique are law enforcement, military intelligence and search and rescue operations.

Such ray-tracing requires a knowledge of the electron distribution with height. A model of the ionosphere would thus benefit both HF communicators and SSL users. There are a number of ionospheric models in existence today, many of which were designed years ago. In the early days of ionospheric modelling and prediction, there was a shortage of ionospheric data in some regions. The databases that the models were based on had to be extrapolated in these areas. In particular, records of ionospheric characteristics in the Southern Hemisphere were found to be sparse or non-existent. Previously, modelling techniques had to be kept simple due to the limited capability of the computer hardware available. Consequently, there are few known ionospheric models available for the Southern Hemisphere.

Both civilian and military users have a strong interest in high-frequency communication and broadcasting via the ionosphere. The reliability of good models of the propagation medium is needed for these users to make efficient use of this natural resource.

This thesis attempts to discover a good model for predicting foF2. Initially, existing models and prediction software are evaluated in order to establish whether there is already a good model for the Grahamstown region or not. Neural networks are introduced as a new approach to solving the non-linear problem of modelling foF2.

Chapter 2

EXISTING MODELS

2.1 Introduction:

Many attempts have been made to model the ionosphere and predict its parameters. Most ionospheric models used for communication predictions are empirical models based on global observations of the ionosphere over the past few decades. This chapter discusses the International Reference Ionosphere (IRI) and SKYCOM, a prediction software package that is based on the IRI. An evaluation was done on both of these models to determine how well they predict the maximum critical frequency of the F2 layer (foF2) for the Grahamstown area.

2.2 The International Reference Ionosphere:

The International Reference Ionosphere (IRI) was introduced in 1969 by a joint working group of the Commitee on Space Research (COSPAR) and the International Union of Radio Science (URSI). This group's aim was to produce an empirical standard model of the ionosphere based on all available data sources. The IRI describes the electron density, ion composition, electron and ion temperatures of the ionosphere for undisturbed magnetic conditions. It provides a

global reference model of these parameters with their temporal mean behaviour. Special IRI workshops are held regularly in order to improve and evaluate the original IRI model.

The IRI can reference one of two different models, the URSI model or the CCIR (International Radio Consultative Commitee) model . Either one of these models can be implemented within the IRI code through the use of numerical coefficients to describe the global behaviour of the ionosphere.

The accuracy of the CCIR model coefficients depends upon the geophysical distribution of the stations whose data were used in the generation of the numerical coefficients. This indicates that in areas where the data was sparse or non-existent, such as the Southern Hemisphere and the ocean areas, the accuracy of the CCIR model coefficients is questionable. The URSI set of model coefficients is essentially an improvement on the CCIR coefficients. Aeronomic theory and spherical harmonic analysis *(Rush et al. [1983])* were used to fill the gaps in the database. The final set of URSI coefficients is a combination of these theoretical values and approximately 45000 station months of ionosonde data.

Some advantages of the IRI are that it is based on all major ionospheric data sources, it produces values of all the most important parameters of the ionosphere, and it has undergone more than a decade of international critical review. One of the limitations of the IRI is that it only gives mean values, the actual values can deviate by up to 30% due to large day-to-day variations. Also, the IRI does not take into consideration any irregularities such as the winter anomaly or spread f that may occur in the ionosphere, and will only allow a sunspot number less than or equal to 150.

Geographical latitude and longitude, date, time and sunspot number are required by the IRI as inputs. It returns the predicted foF2 value or maximum electron density of the ionosphere at that position under the specified set of conditions.

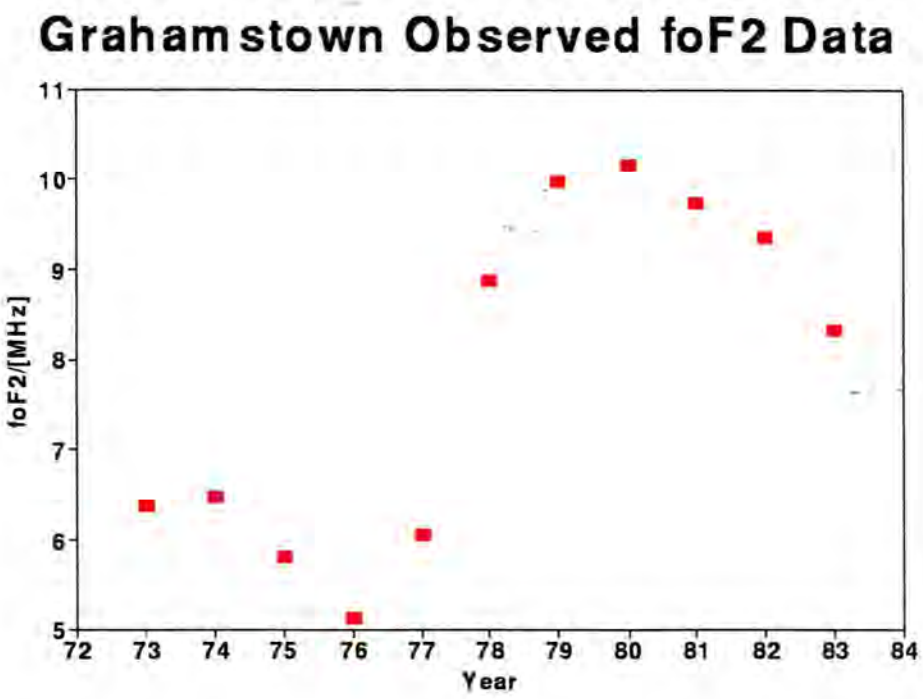

Figure 2-1: The mean observed Grahamstown foF2 values for July of each year.

The IRI was set up to predict foF2 (in MHz) for Grahamstown over a certain period of time. These predicted values were then compared with the actual measured values in order to establish how the IRI performs in the Grahamstown region. As an indicator of prediction accuracy the root mean square (rms) error value was calculated. Initially, the 12 noon South African Standard Time (SAST) values for a winter month, July, over one complete solar cycle, 1973 to 1983, were predicted. The monthly mean foF2 values observed for Grahamstown are shown in figure 2-1. For the sunspot number (SSN) input the documentation on the IRI suggests the 12 month running mean value (R12). However, results obtained from using the 1 month running mean value (R1) produced a lower rms error value and an overall better fit to the measured data *(Williscroft and Poole [1995])*. The observed foF2 values and the predicted values obtained from using both R12 and R1 are shown in figure 2-2. The R1 value was used as the SSN input for the remainder of the IRI analysis. Using the R1 value and taking the average noon foF2 value for July, predicted and observed, the rms error was 0.35 MHz.

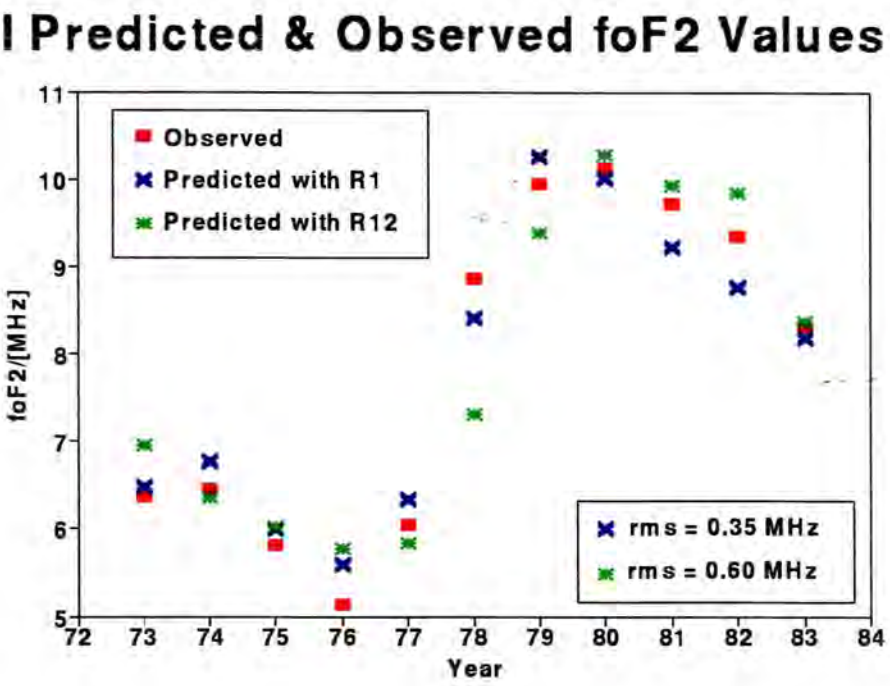

Figure 2-2: This graph shows the mean observed and predicted values for July of each year. The IRI predicted values obtained from using R12 and those from using R1 are shown with their respective rms error values.

To further test the IRI the data set was extended to include all the 12 noon SAST Grahamstown data from 1973 to 1983. The IRI prediction for the daily 12 noon foF2 value was obtained. Figure 2-3 shows the IRI predictions for two years from different points in this sunspot cycle, 1976 (low sunspot cycle) and 1980 (high sunspot cycle). The rms error between the observed and predicted values for the entire period, 1973 to 1983, was 1.55 MHz.

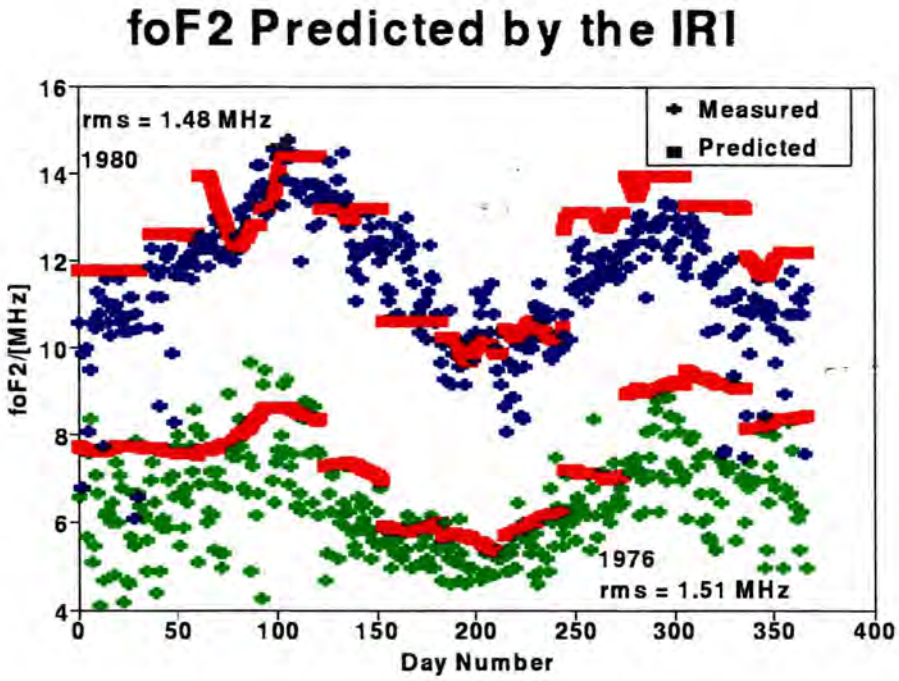

Figure 2-3: This graph shows the observed foF2 values and those predicted by the IRI for a year at high sunspot cycle (1980) and a year at low sunspot cycle (1976).

2.3 SKYCOM:

SKYCOM is a high-frequency ionospheric signal analyst which was developed by the Solar-Terrestrial Dispatch and released in 1994. This computer program provides a prediction service that claims to be flexible enough to handle most geophysical conditions. SKYCOM can compute electron density profiles, ionospheric characteristics and global ionospheric maps. It can also perform ray-tracing for applications such as the single-site location discussed in chapter 1.

SKYCOM is based on the IRI, but has the extra feature of using some level of the magnetic activity as one of its inputs. The date, time, transmitter and receiver location, an indicator of solar activity and a magnetic index are used as inputs to the program. The solar activity indicator can be either the sunspot number or the 10.7cm solar radio flux value, while the magnetic index is the A-Index value.

The 12 noon SAST foF2 value (in MHz) for Grahamstown was predicted by SKYCOM for July of every year from 1973 to 1983. Based on the findings of *Williscroft and Poole [1995]* the R1 value was used as the sunspot number (SSN) input. The daily A-Index was used for the magnetic index as required by SKYCOM. The values were averaged over each month and the rms error between the observed and predicted monthly averages was calculated to be 0.46 MHz. Figure 2-4 is a graph of the observed and predicted foF2 values from SKYCOM.

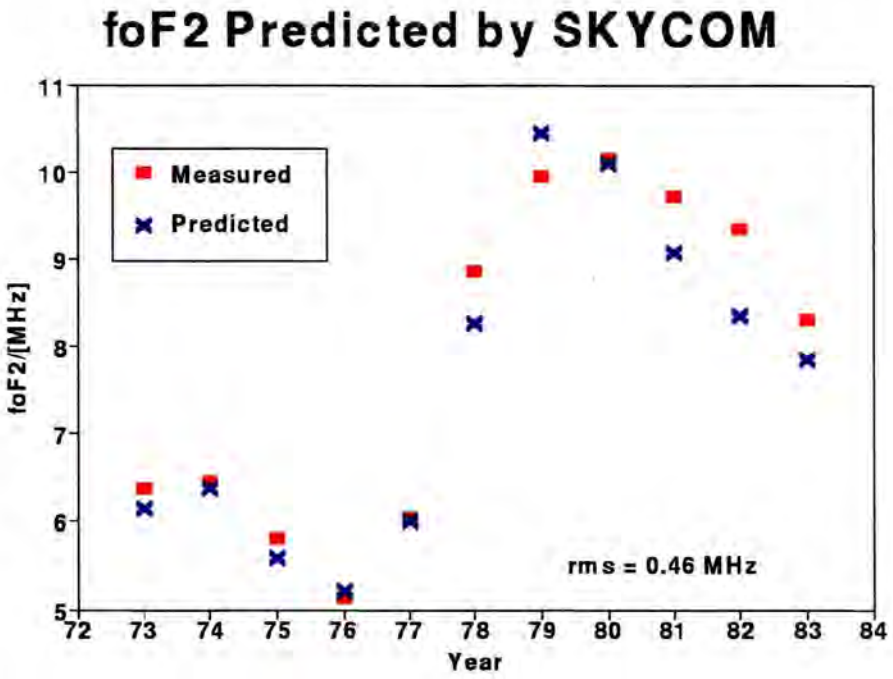

Figure 2-4: The mean observed foF2 values are shown with those values predicted by SKYCOM for July of each year.

2.4 Conclusion:

It has been known for a long time that there exists a relationship between the SSN and foF2. The foF2 value increases at times of high sunspot number and decreases at times of low sunspot number. When predicting foF2, the IRI first takes the month into account and then makes some adjustment for the SSN. Should the SSN be higher than 150 for an entire month the IRI predicts foF2 to be constant for that month. This explains the shape of the IRI predicted graph shown in figure 2-3 and may result in IRI predictions being weak in the Grahamstown area.

SKYCOM is based on the IRI but makes some allowance for the level of magnetic activity. It has already been mentioned that the R1 value of the SSN was found to be a better predictor of foF2 for the Grahamstown region than the suggested R12 value. The same could apply to the A-Index. A recommended value of the A-Index for use with SKYCOM is the daily A-Index value. This A-Index may not be the best predictor of foF2 at noon since it is evaluated retrospectively based on the K-Indices for the whole day and therefore includes information that is ahead of the 12 noon coordinate. A re-defined A-Index that is based on observed information from before 12 noon may prove to be more accurate for the prediction of foF2.

The best rms error on the monthly mean data was 0.35 MHz for values predicted by the IRI. For daily predicted values of foF2 the rms error was 1.55 MHz. The criterion for a model of foF2 to be an improvement on these models is a reduction in the rms error value. The purpose of the research discussed in this thesis is to find an improved model of foF2 for the ionosphere over Grahamstown and the rest of South Africa.

Chapter 3

A TRADITIONAL APPROACH

3.1 Introduction:

A traditional approach to the problem of prediction is the method of linear regression *(Mosteller and Tukey [1977])*. Regression methods illustrate the relationship between variables. Linear regression is commonly used for prediction although it can be used to solve many other problems as well.

The purpose of this thesis is to find a model for the maximum electron density (foF2) of the ionosphere over Grahamstown. This chapter discusses the use of the traditional method of linear regression to investigate the dependence of foF2 on day number, sunspot number (SSN) and magnetic A-Index (AI). This investigation has been split into two sections. The first section deals with the dependence of foF2 on the SSN and AI only while the second section investigates the dependence of foF2 on the day number alone. The spreadsheet software package, QuattroPro 3 *(Borland International, [1991])*, has the ability to do linear regression on any given set of variables. This feature was used extensively for the work done in this chapter.

3.2 Regression Analysis:

3.2.1 Dependence of foF2 on SSN and AI:

Initially this analysis concentrated on the SSN and AI parameters and how they affect the value of foF2. Monthly mean values of foF2 for only one month, July, were considered which allowed the day number to be excluded. Linear Regression was used in an attempt to predict these foF2 values over 1 solar cycle *(Williscroft and Poole [1995])*. In chapter 2 the International Reference Ionosphere (IRI) was used to predict the same values and the result obtained from that experiment is used here as a comparison. Figure 3-1 shows the monthly mean foF2 values for July as predicted by the IRI and how they compare to the measured values.

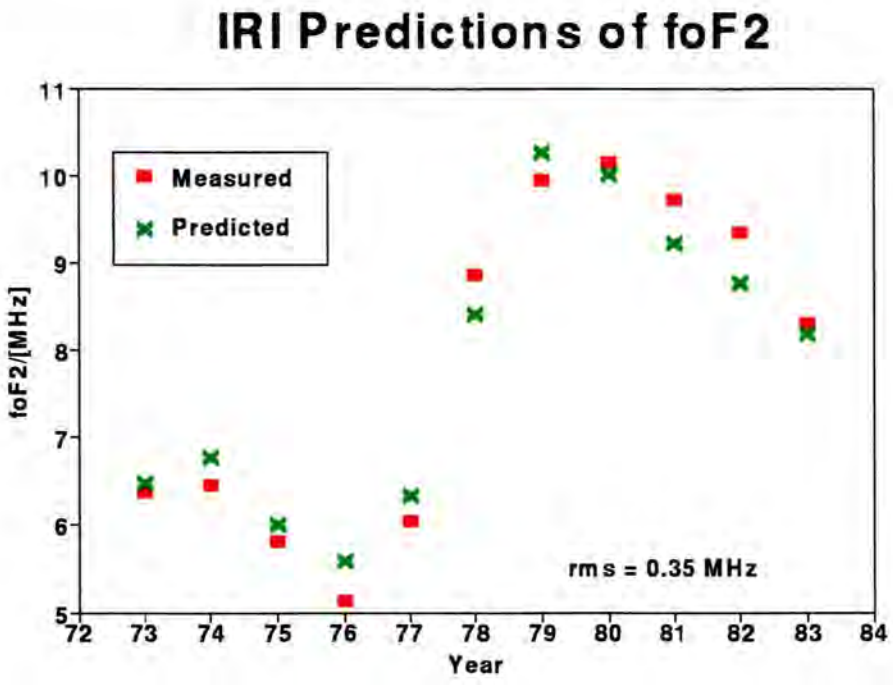

Figure 3-1: The 12 noon monthly mean foF2 values predicted by the IRI and the measured monthly mean foF2 values for July of 1973 to 1983. The rms error was 0.35 MHz.

The independent variables used in the regression were the 1 month running mean SSN (R1) and the daily AI value. The analysis was done for three separate regression equations.

The first analysis assumed the form

$$foF2 = C + m_1 * (SSN) \tag{3-1}$$

where m_1 is the coefficient of the first variable and C is the constant term. This gave a reasonable fit and, when compared with the measured values, a rms error of 0.29 MHz. An AI term was then included.

$$foF2 = C + m_1 * (SSN) + m_2 * (AI) \tag{3-2}$$

where m_2 is the coefficient of the second variable. The rms error between the foF2 values predicted by equation 2 and the measured values was 0.23 MHz. Including the AI term has caused an improvement in the predicted values of foF2 as seen by the reduction in the rms error.

The third equation included a cross term of the product of the SSN and the AI.

$$foF2 = C + m_1 * (SSN) + m_2 * (AI) + m_3 * (SSN * AI) \tag{3-3}$$

The fit of the predicted values to the measured values improved further with the addition of this term. The rms error was 0.21 MHz. The equivalent rms errors obtained from the IRI and each of the three regression equations are tabulated in table 3-1.

RMS ERRORS/[MHz]	
Model	**RMS**
IRI	0.35
Equation 1	0.29
Equation 2	0.23
Equation 3	0.21

Table 3-1: Rms errors, in MHz, for predictions of monthly mean foF2 values using each of the models considered.

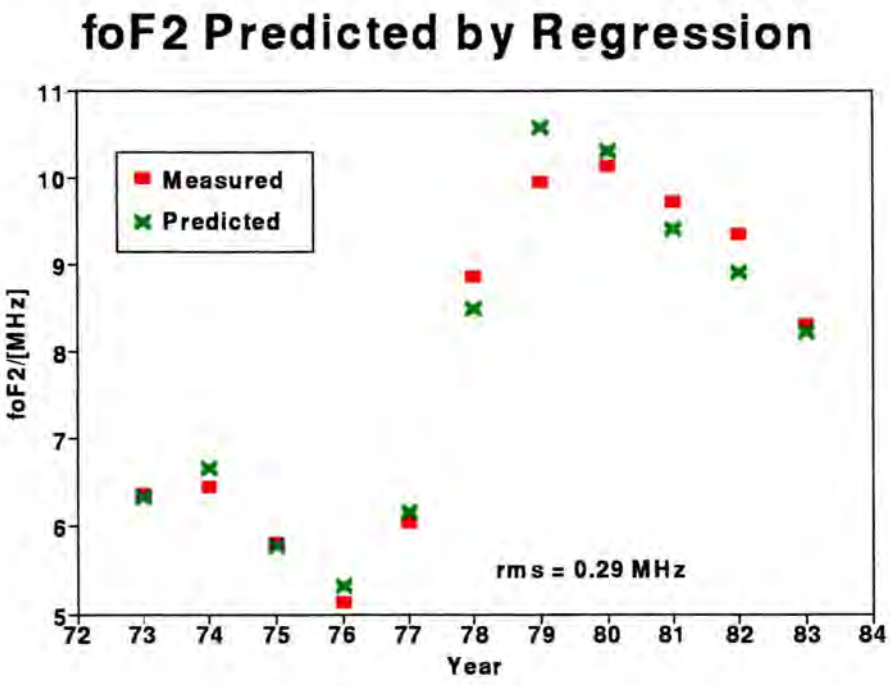

Figure 3-2: Monthly mean predicted foF2 values from regression analysis of the form represented by equation 3-1, and the measured values for each year.

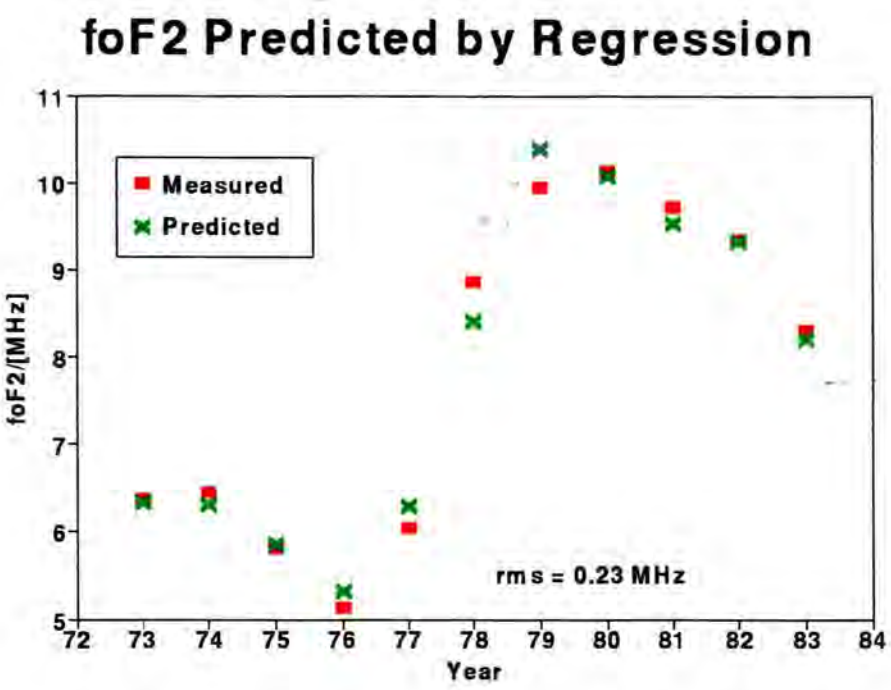

Figure 3-3: Monthly mean predicted foF2 values from regression analysis of the form represented by equation 3-2, and the measured values for each year.

The graphs of the foF2 values predicted by the regression equations and the measured values are illustrated in figures 3-2, 3-3 and 3-4 respectively. It can be seen from these graphs that the fit improves as additional terms are added. A common factor in all three is that although the fit is accurate on the falling side of the sunspot cycle there are large errors on the rising side of the cycle. These errors are, at the present time, unexplained.

The results obtained from this regression analysis show a strong dependence of the foF2 value on SSN and a somewhat lesser dependence on the AI value.

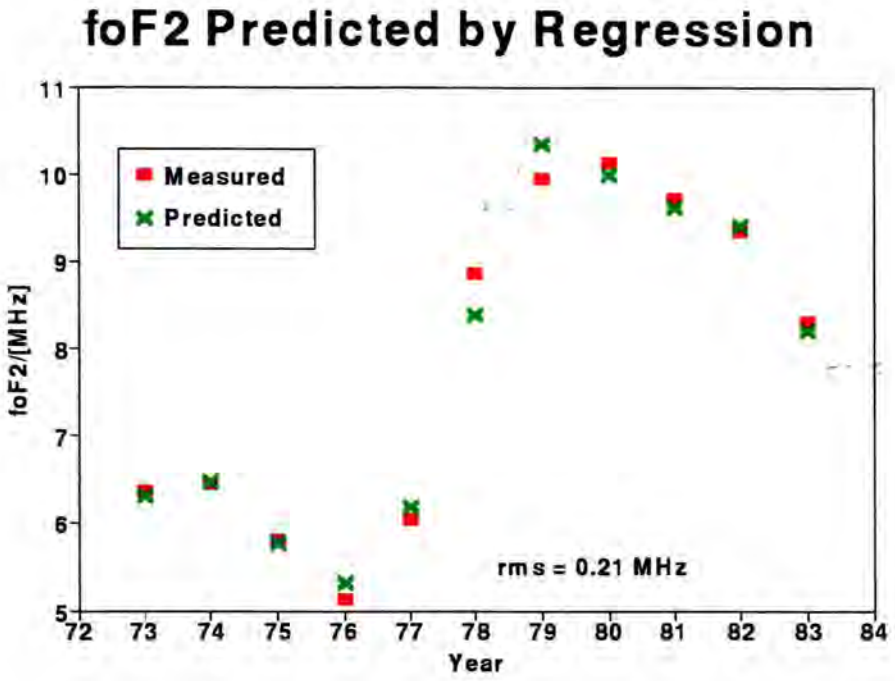

Figure 3-4: Monthly mean predicted foF2 values from regression analysis of the form represented by equation 3-3, and the measured values for each year.

3.2.2 Dependence of foF2 on day number:

Up until this point in the investigation the seasonal dependence of the foF2 value on the day number was not taken into account. Fourier Analysis was used in an attempt to predict the variation of foF2 from its dependence on the day number (D) for one year of data. This equation took the form

$$foF2(D) = \sum_{n=1}^{m} [A_n cos(\frac{2\pi Dn}{365}) + B_n sin(\frac{2\pi Dn}{365})] \qquad (3\text{-}4)$$

The coefficients, A_n and B_n, were found by applying a linear regression with the cos and sin terms as the independent variables and the foF2 value at 12 noon on day D as the dependent variable. This analysis was applied to one year at solar maximum (1981) and one year at solar minimum (1974). Equation 3-4 was expanded to the 5th harmonic ($m = 5$) and the results obtained for these two years are represented by the graphs shown in figure 3-5. The rms errors obtained for 1974 and 1981 were 0.87 MHz and 1.04 MHz respectively.

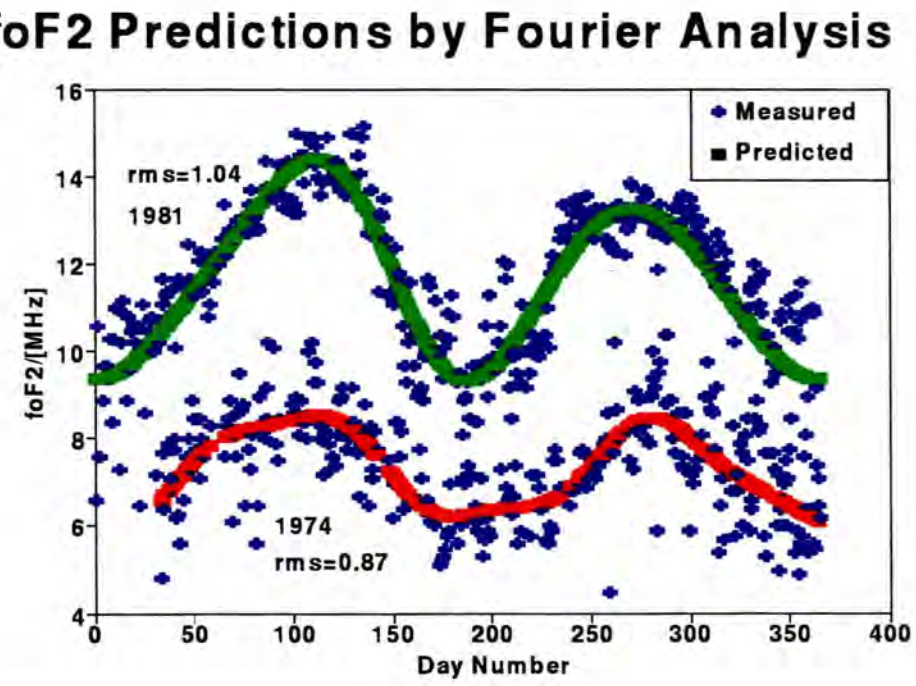

Figure 3-5: This figure shows the fit of the predicted foF2 values, as obtained from Fourier analysis on the day number, to the measured foF2 values. The analysis was done for one year at a time only and a comparison is made between solar minimum (1974) and solar maximum (1981).

In comparing the 1974 and 1981 predictions it can be seen that the coefficients obtained for each of these years are somewhat different.

3.3 Conclusion:

It has been shown in this chapter that foF2 does depend on the day number, the sunspot number and the A-Index. This investigation was done in two sections. The results obtained from each of these sections would need to be combined into one model for predicting the 12 noon value of foF2. To achieve this the A_n and B_n coefficients of equation 3-4 could be made SSN and AI dependent. This would involve a multivariable regression that is reliant on guessing the optimum variables to be used in the final equation. The result of this would be an extremely complicated modelling equation that involves many terms.

A model of the ionospheric parameter, foF2, needs to be simple and must take into account all the parameters that influence foF2. It must also be easily expandable and perform well in any sunspot cycle and at any time. The next few chapters discuss a new method for modelling foF2 that meets these, and other, requirements and produces results which are a significant improvement on the results seen thus far.

Chapter 4

NEURAL NETWORKS

4.1 Introduction:

A Neural Network (NN) is an information processing system that is designed to perform in a way that is similar to the operation of the human brain. Essentially, the NN is a computer programme that can be trained by presenting to its input any number of multi-dimensional input vectors that correspond to a known measured parameter. The NN will learn to identify the relationship between the input vectors and the known output parameter in much the same way that a child will learn to recognise the letters in the alphabet.

The purpose of this chapter is to introduce the concept of neural networks and to provide background information that is required for the research presented in the following chapters. A NN can be identified by its different properties. The properties that have been implemented in the NN that was designed to do the work set out in this thesis are discussed here.

4.2 A Single Node and Activation Function:

A NN is made up of many processing elements called nodes. Each node sums its weighted input signal and applies an activation function to determine its output signal. A typical node with its input and output signal processes is shown in figure 4-1. There is always a constant input, called a "bias", equal to 1 which ensures that the output of the node operates around a zero mean.

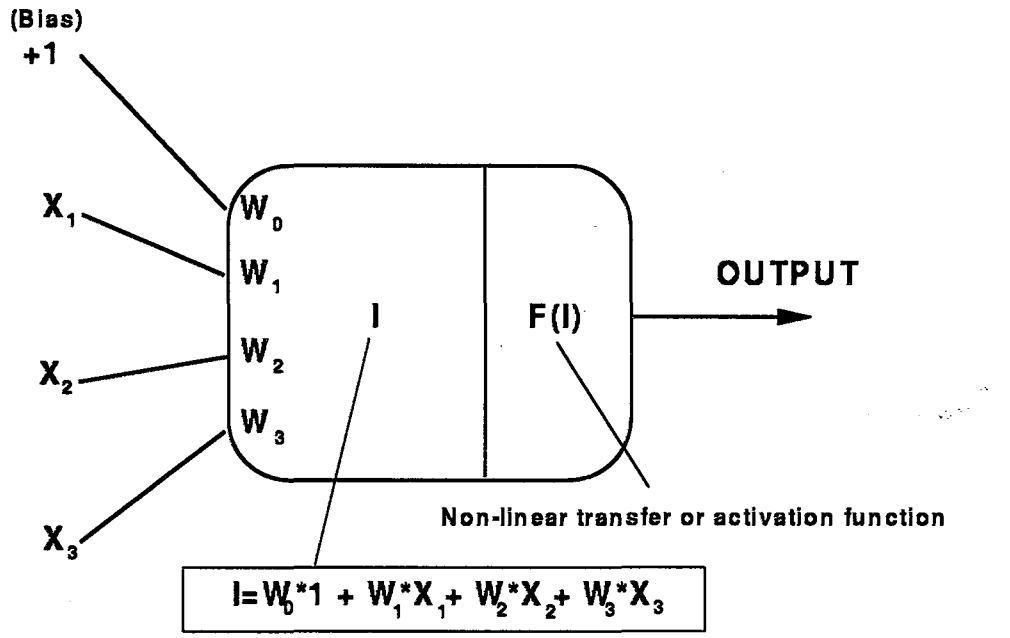

Figure 4-1: Illustration of the operation of a node. The weighted inputs are summed and then applied to an activation function to determine the output.

The activation function is usually non-linear and the same for all nodes in any particular layer of the NN. A bipolar sigmoid function, shown in figure 4-2, is most often used in NN's trained with the back-propagation algorithm. The bipolar sigmoid function has a range (-1,1) and is defined as

$$f(x) = \frac{1 - exp(-\sigma * x)}{1 + exp(-\sigma * x)}$$

where σ is the steepness parameter. The hyperbolic tangent function, tanh, is closely related to the bipolar sigmoid function and is often used as an activation function.

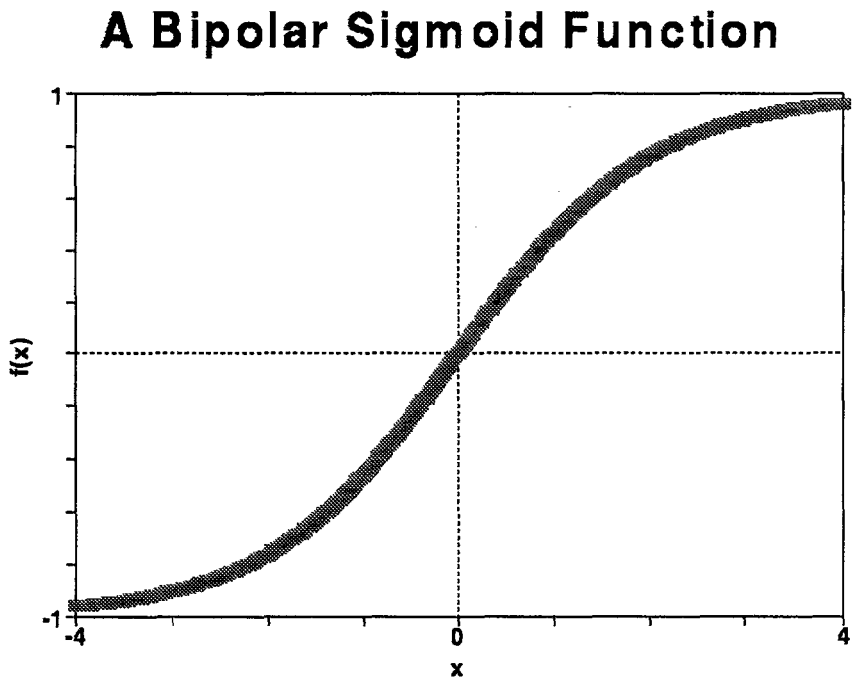

Figure 4-2: A graphical example of the bipolar sigmoid function with range from -1 to +1.

4.3 The Architecture:

The architecture of the NN is made up of nodes arranged into layers and connected together through weighted communication links. NN's can be classified as either single-layer or multi-layer. A single-layer net has only input and output nodes whereas a multi-layer net has a number of hidden layers as well. An example of a multi-layer net is shown in figure 4-3. Multi-layer nets are able to solve complicated problems that cannot be solved by a single-layer net. The hidden layers present in these nets lie between the input and output layers and consist of a number of hidden nodes. A NN with only one hidden layer is usually sufficient to solve most problems *(Fausett, [1994])*. The number of hidden nodes present in a hidden layer is characteristic of the NN being used.

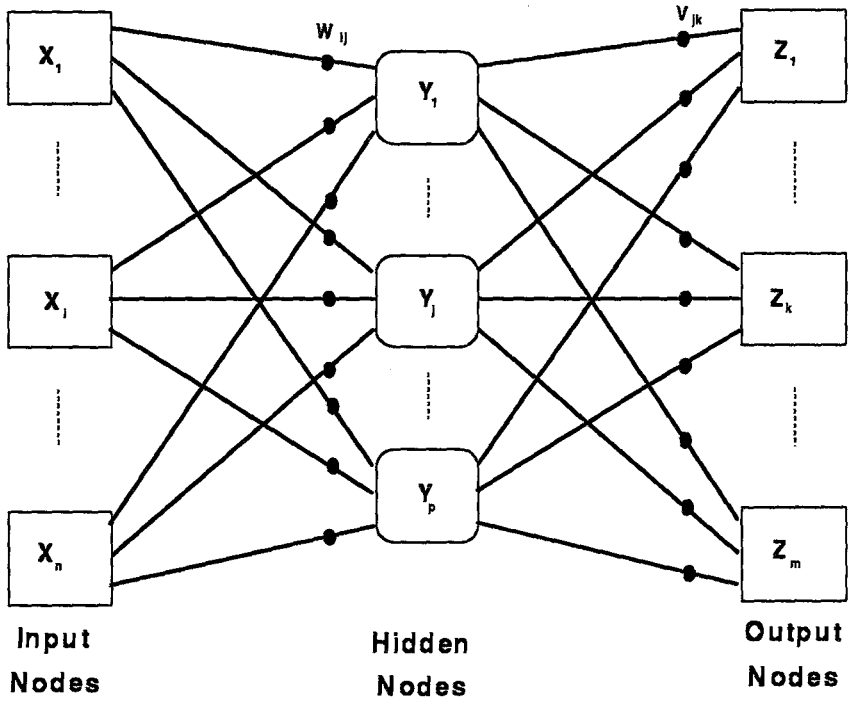

Figure 4-3: An example of a multi-layer neural net with 1 hidden layer. The W_{ij} are the weights from the input to the hidden layer and the V_{jk} are the weights from the hidden to the output layer.

It is common to fix the number of hidden nodes in the hidden layer. However, a constructive method can be used to determine the number of hidden nodes required. This method is referred to as a cascaded learning architecture *(Haykin, [1994])*. The NN starts off with no hidden nodes and then adds them one or a few at a time. Each new node has a weighted connection from each input and from each of the previously added nodes. New nodes are continuously added until such time as the rms error has stabilised.

4.4 The Learning Process:

A characteristic of different NN's is the method used for determining the values of the weights within the NN. This method is referred to as the learning process or training process.

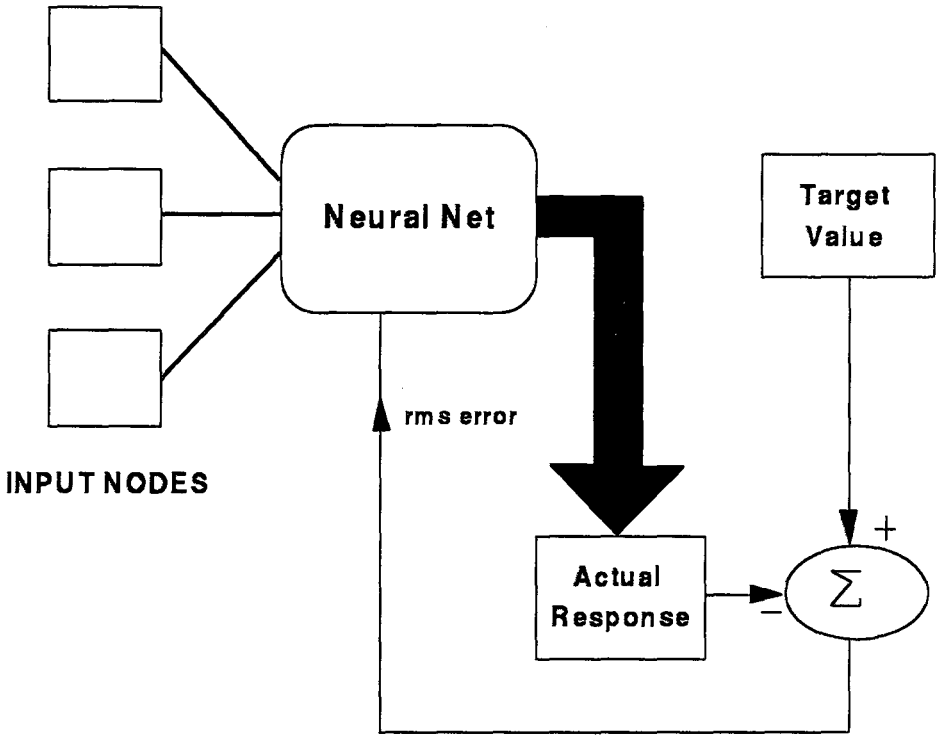

Figure 4-4: A block-diagram of the supervised learning algorithm. The $\sum$ symbolises the operation of finding the rms difference between the target value and the actual response.

One of the most common learning processes is that of supervised learning. The NN is presented with a set of inputs that correspond to a known measured parameter, the target value. This target value represents the optimum result the NN should aim for given that particular set of inputs. The actual response of the NN is determined and the rms error is calculated. The NNs weights are then adjusted iteratively in such a way as to reduce the rms error. When the rms error has stabilised, the NN has completed its task to the best of its ability under the set of conditions specified. The NN can then be presented with inputs of the same type that it has never seen before and it will predict the output response. This is known as the testing process. Figure 4-4 is a block- diagram of the supervised learning algorithm. A generalised example is the back-propagation algorithm. The error-terms in this algorithm are back-propagated through the network on a layer-by-layer basis.

4.5 Conclusion:

There are a few commercial neural network software packages available today. For the research presented in this thesis a software package called *Predict (NeuralWare release A11 [1995])* was used. *Predict* uses a cascaded architecture combined with direct input-output links. The final architecture had 4 inputs, 17 hidden nodes and 1 output. A feed-forward back-propagated learning algorithm was implemented. The activation function on the hidden nodes was a tanh function and on the output node it was a sigmoid function. The architecture for this NN is shown in figure 4-5 and will be discussed further in the next few chapters.

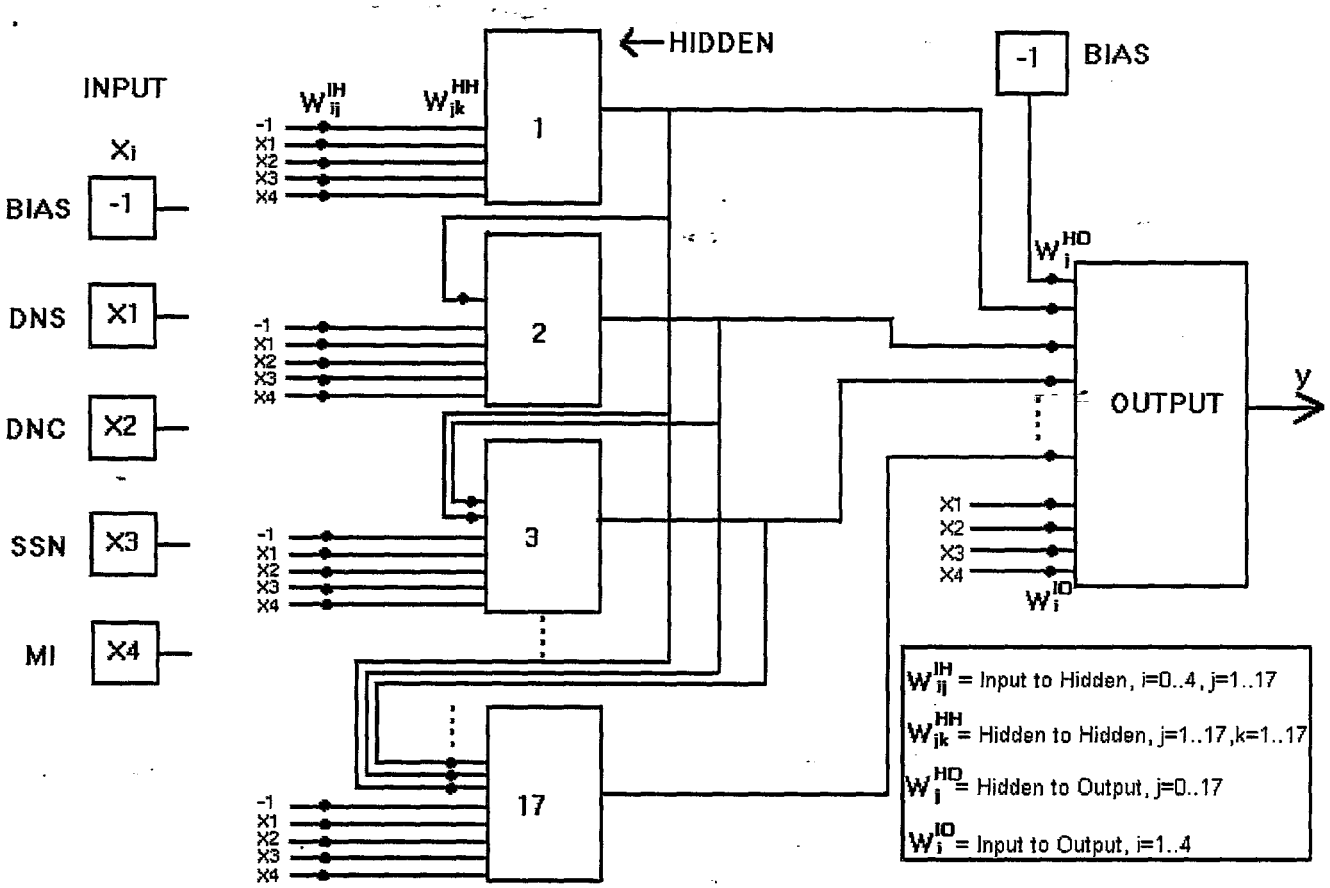

Figure 4-5: This diagram represents the architecture of the neural network used for the research presented in this thesis. The black dots represent the weighted links as indicated in the key.

Different problems will require different NNs to solve them. The result from any NN may be improved by changing any number of the NN's characteristics. For example, a different learning rule, fixed hidden nodes or a different initialisation point may be used. *Haykin, [1994]* and *Fausett, [1994]* both give suggestions as to ways in which to improve a net.

This chapter has discussed the special cases of each property that have relevance to the work presented in this thesis. The next two chapters will discuss how a NN was trained to predict the maximum electron density of the ionosphere.

Chapter 5

DETERMINING THE BEST PREDICTORS OF foF2

5.1 Introduction :

The critical frequency of the ionosphere, foF2, is a measurable quantity that represents the maximum ionospheric electron density. The ionosphere is a propagation medium that varies with time, season, longitude, latitude, solar activity and magnetic activity. All of these variations must be taken into account when predicting foF2.

This thesis attempts to find a model for the 12 noon value of foF2 over Grahamstown, South Africa (26°E, 33°S). The aim of this chapter is to set up the input parameters needed for predicting foF2 and to show how a neural network (NN) can be used as a tool when determining input parameters.

5.2 Using a Neural Net :

A NeuralWare software package called *Predict* (*NeuralWare release A11, [1995]*) was used to train the NN. One solar cycle of data, 1973 to 1983; was presented to the NN. Each of the 3541 vectors consisted of a 4–dimensional input and a corresponding known output. The known output was the 12 noon foF2 value for Grahamstown. The 4–dimensional input was made up of the cyclic components of the day number, a measure of the solar activity and a measure of the magnetic activity. These inputs are dealt with in more detail later in this chapter. From the original data set of 3541, 70% were used for training and 30% for testing the NN. This division of the data set prevents overtraining and ensures generalisation of the result. The NN trains until the rms error between the measured and predicted foF2 values on the testing set has stabilised. Figure 5-1 is a schematic diagram of the NN used in this chapter.

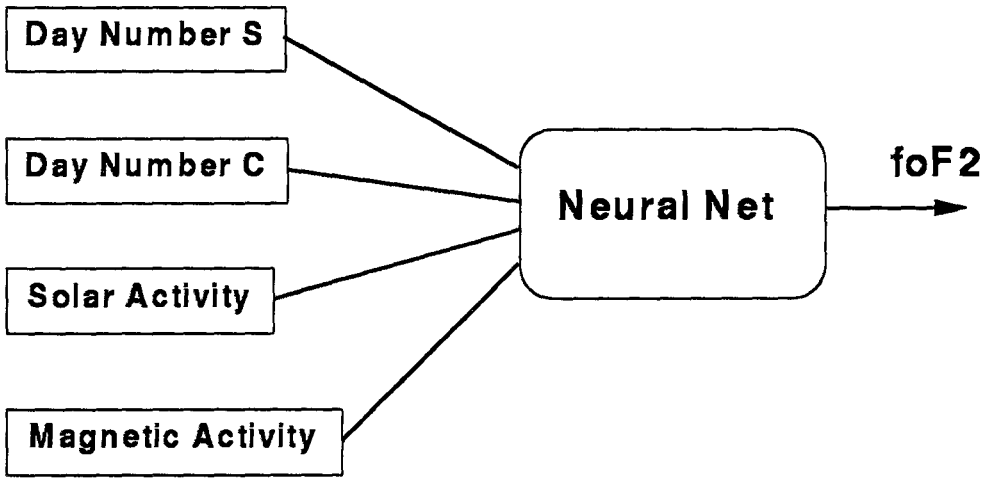

Figure 5-1: This diagram is a schematic drawing of the generalised inputs to the NN refered to in this chapter.

5.3 Input Data :

In order to predict the 12 noon foF2 value over Grahamstown suitable representations of the seasonal variation, the solar activity and the magnetic activity need to be found. The diurnal and geographic location variations have been eliminated by choosing one hour of the day and a particular location.

5.3.1 Day Number :

The seasonal variation can be described by the day number (DN) which is an integer in the range 1 to 365. One of the problems with DN is that although December 31 and January 1 are temporally adjacent they are numerically far apart. However, this can be solved by splitting DN into two inputs, DNS and DNC, where

$$DNS = sin(\frac{2\pi * DN}{365})$$

$$DNC = cos(\frac{2\pi * DN}{365})$$

Together DNS and DNC provide cyclic continuity across the year end boundary.

5.3.2 Solar Activity :

The parameter foF2 depends partly on the flux of ultraviolet radiation from the sun. Therefore, an average measure of the solar activity needs to be included in the set of inputs used to determine foF2. There are two solar activity parameters available, the daily sunspot number and the 10.7cm solar flux. In this chapter, NNs have been implemented for the first time to determine the optimum length of time over which these parameters should be averaged and which one of the two is a better predictor of foF2. The sunspot number shall be refered to as SSN and the solar flux input as SFX.

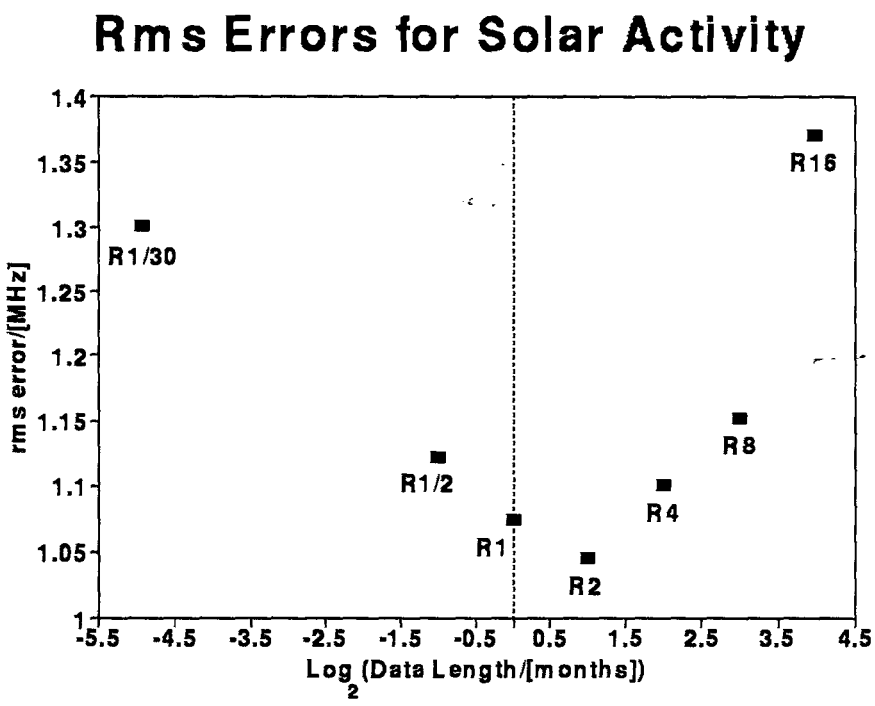

Figure 5-2: This diagram depicts the rms error between the measured and predicted values of foF2. The rms errors apply to 7 different NNs trained with running means of SSN of length $\frac{1}{30}$, $\frac{1}{2}$, 1, 2, 4, 8, and 16 months. The optimum period over which to average the SSN appears to be 2 months (*after Williscroft and Poole, [1996]*).

Seven different NNs were trained and tested with running means of daily sunspot number over the preceding $\frac{1}{30}$, $\frac{1}{2}$, 1, 2, 4, 8, and 16 months. A new solar activity index, called RX, is defined, where X is the number of months over which the daily sunspot number was averaged. The value of SSN used in the NN that gave the minimum rms error obtained on the testing set was taken to be optimum. The input representing magnetic activity was left out of the input set for the solar activity tests. Figure 5-2 shows the rms errors obtained for each of these NNs. It can be seen that the SSN value should be an average over a period of approximately 2 months (SSN=R2).

Similarly, several NNs were trained with running means of daily solar flux values as the measure of solar activity. A direct comparison of the rms errors obtained from using the SSN value and using the SFX value is shown in figure 5-3. From this graph it appears that the SSN value is marginally the best indicator of solar activity that should be used for the prediction of the 12 noon foF2 value. For the remainder of the research presented in this chapter, the R2 value of the SSN is used.

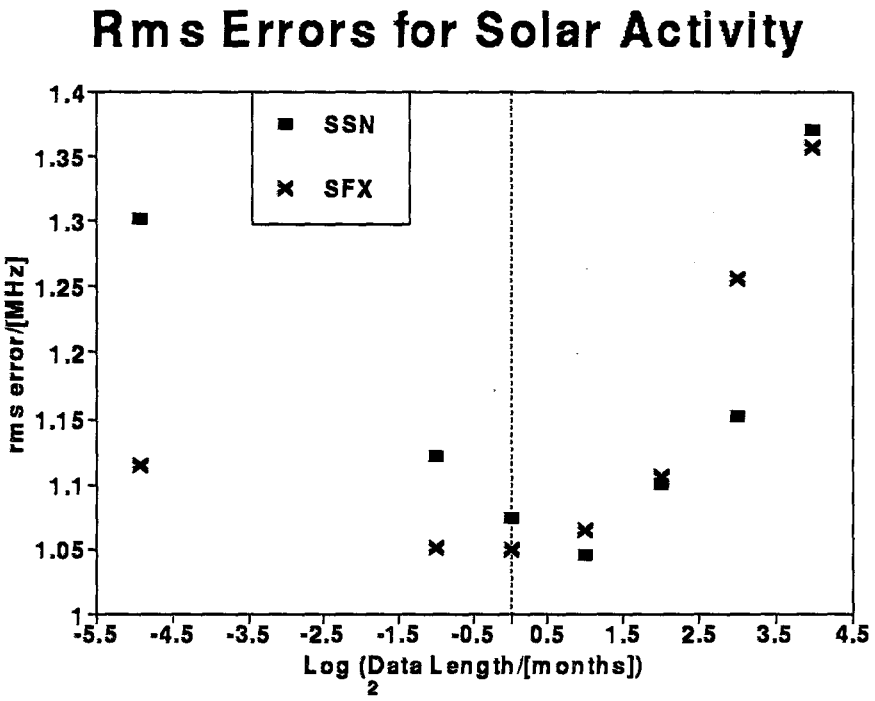

Figure 5-3: This diagram depicts the rms errors between the measured and predicted values of foF2. Both the rms errors for SSN and SFX at different data lengths are shown.

K	0	1	2	3	4	5	6	7	8	9
a_k	0	3	7	15	27	48	80	140	240	400

Table 5-1: Equivalent a_k values for a given K.

5.3.3 Magnetic Activity :

Magnetic activity can be represented by a variety of indices (*Matsushita and Campbell, [1967]*). The magnetic K-Index is readily available. As with SSN there is a need to find an optimum length over which to average this index. The input that represents the level of magnetic activity shall be referred to as MI.

The K index is an integer in the range 0 to 9 which gives an indication of the intensity of irregular geomagnetic activity in three-hour intervals. Table 5-1 shows the look-up table used by magnetic observatories to convert this K index into an equivalent a_k value. The magnetic data used in this research has been obtained from the Hermanus Magnetic Observatory. The arithmetic mean of the eight a_k indices for the day is referred to as the daily A_k index.

Two magnetic indices were defined for the research presented in this chapter. The first is an average of the K indices while the second is an average of the a_k indices preceding the hour of interest. These have been named WX and AX indices respectively, where X is the number of 3-hour intervals over which the averaging takes place.

The optimum MI value was arrived at in much the same way as the optimum SSN value. Four different NNs were trained using the WX value as the MI value. X was set to 4, 8, 16 and 32. The SSN input for these NNs was set to the R2 value. Similar NNs were trained with MI=AX. A16 was found to be the optimum MI input. Figure 5-4 shows the rms errors from both the AX NNs and the WX NNs. These rms errors are on the testing data set only.

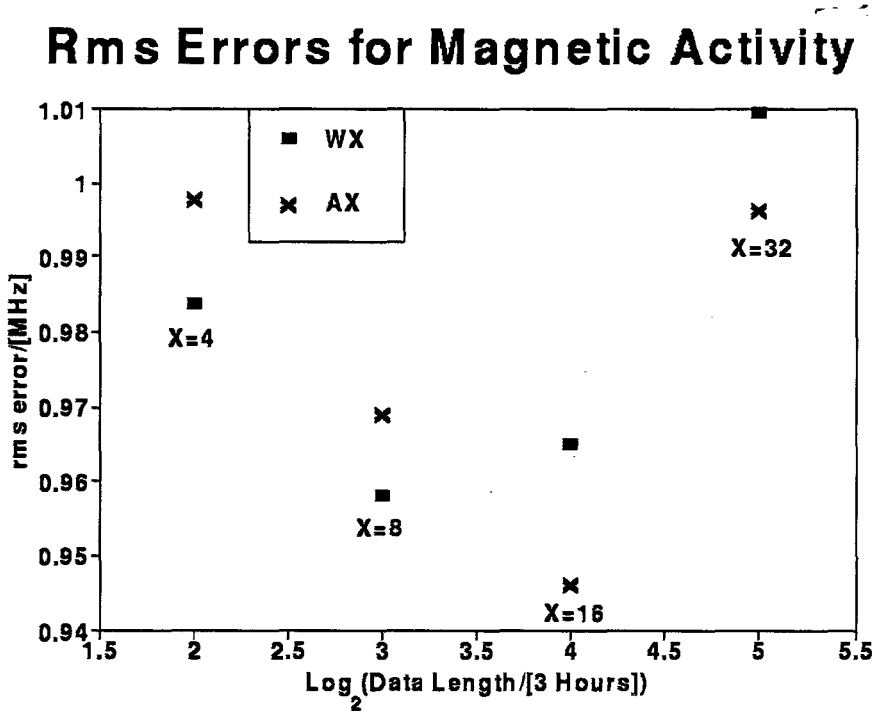

Figure 5-4: This diagram illustrates the rms errors between the measured and predicted values of foF2. The rms errors apply to 4 different NNs trained with the different A and W indices as indicated. The optimum value appears to be A16.

5.4 Conclusion :

The ionospheric parameter foF2 is dependent on many variables. In this chapter foF2 has been limited to the 12 noon value for Grahamstown, thereby eliminating the time of day and location variables. The remaining variables were then considered.

Solar activity can be measured by either the daily sunspot number or the 10.7cm solar flux. A NN was used to find the optimum averaging length for these parameters. It was found that the best solar predictor of foF2 is the 2-month running mean sunspot number. This is in contrast to the International Reference Ionosphere (IRI) (*Bilitza, [1990]*), which has always recommended the 12 month running mean sunspot number.

The 2-day average A index value for the magnetic activity was found by a similar method. The K index is a logarithmic scale and the a_k index is a linear scale that attempts to transform the K index to values that are more acceptable for statistical manipulation. An average of a_k indices gives the A Index. Therefore, what has been defined here as the AX index is a transformed value of the similarly defined WX value. The AX index is suitable for statistical manipulation and this would explain the reason for AX index being optimum. Figure 5-2 shows the rms errors from the NNs trained with RX values in the input, but without the MI input. The minimum value was 1.046 MHz for R2 alone. By comparing this value with the rms error of 0.946 MHz for R2 plus A16, in figure 5-4, it can be seen that an improvement of 10.8% was achieved by including the MI input. This was a major finding of this research as it justifies the inclusion of MI for the prediction of foF2.

The research presented in this chapter is the subject of a paper that has been accepted for publication in Geophysical Research Letters. Chapter 6 of this thesis deals with using a NN to predict foF2, given R2 as the SSN input and A16 as the MI input.

Chapter 6

TRAINING A NEURAL NET TO PREDICT foF2

6.1 Introduction:

In the past, many attempts have been made to model the ionosphere using seasonal and sunspot information. One of the most popular models available is the International Reference Ionosphere (IRI) (*Bilitza, [1990]*). This thesis makes use of the IRI as a benchmark for comparison with the newer model being investigated.

The previous chapter dealt with the use of neural networks (NNs) to determine the optimum parameters required for predicting the maximum electron density in the ionosphere (foF2). This chapter deals with the new application of NNs, using these parameters, to foF2 prediction.

6.2 Programming the Neural Net:

A NeuralWare software package called *Predict* (*NeuralWare Release A11 [1995]*) was used to train the NN by repeating the training process from different starting points. Each time the NN begins its training it chooses different initial random values for its weights. *Predict* uses the entire data set to find the best possible route to a well trained NN. There are a number of different parameters within the program which allow the user to assist *Predict* in finding this route.

Initially, each input is transformed to lie between the values -1 and +1. Although a number of different transformations of the input data was possible, the degree of transformation was set to "scale data only". This instruction allowed the program to make only the minimum changes to the data. The amount of noise in the data was pre-set to "moderately noisy data". *Predict* also has the ability to select only those variables that make a significant difference to the outcome. For the NN used to predict foF2 this feature was disabled ("no variable selection").

6.3 Training the Neural Net:

The NN is trained by presenting to its inputs any number of multi- dimensional training vectors which correspond to a known measured parameter. The NN compares its output to the known parameter and applies an iterative correction to its internal weights to minimise the difference.

A 4-dimensional set of input vectors corresponding to 1 solar cycle (1973 to 1983 inclusive) of 12 noon values of foF2 was presented to the NN. The input vector consisted of the sine and cosine components of the day number (DNS, DNC), the 2-month running mean sunspot number (R2) and the 2-day averaged A-index (A16) as discussed in the previous chapter. Figure 6-1 is a schematic diagram of the inputs presented to the NN and the corresponding output.

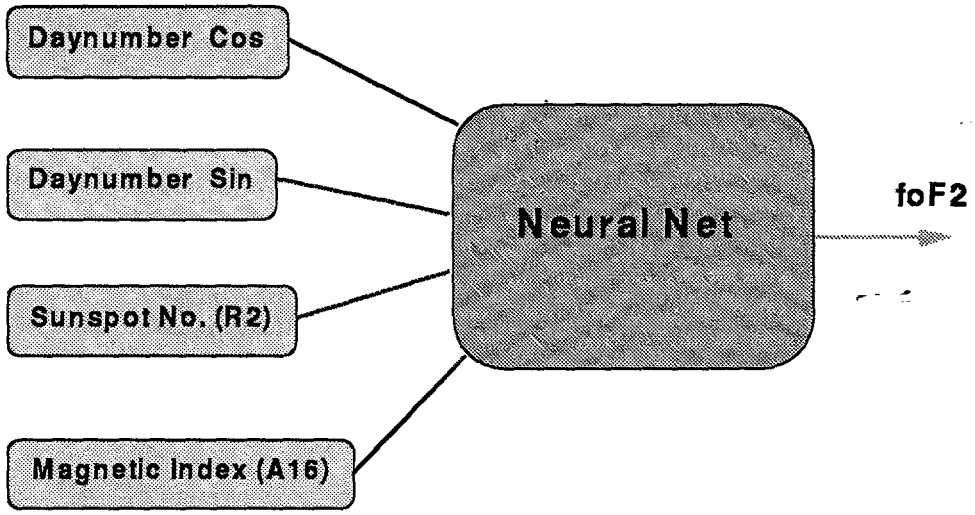

Figure 6-1: A schematic diagram of the inputs presented to the NN for training and the corresponding output.

The final NN architecture, which was arrived at according to the procedure described in chapter 4, consisted of 4 inputs, 17 hidden units and 1 output unit. A diagram of this architecture appears in chapter 4.

Of the original data set of 3541 vectors, 70% was used for training and 30% for testing the NN. The testing data set is used to check on the progress of the training phase. This prevents overtraining of the NN and ensures generalisation of the result. When the rms error between the predicted and measured values of the testing set has stabilised the NN stops training.

6.4 Results:

All of the diagrams that appear in the remainder of this chapter refer to the testing data set only. The results are shown in figure 6-2a and figure 6-2b. The output data are presented

RMS ERRORS/[MHz]			% Improvement
Year	**NN**	**IRI**	$\frac{(IRI-NN)}{IRI} * 100$
1973-1978	0.85	1.42	40.1%
1978-1983	1.03	1.66	40.0%
1989	1.03	1.75	41.1%
1995	0.92	1.68	45.2%

Table 6-1: The rms errors, in MHz, between the measured and predicted foF2 values are tabulated above.

chronologically along the x-axis. Both the measured and the predicted values are shown. Figure 6-3 shows two years taken from the same data set, a year at solar maximum (1980) and a year at solar minimum (1976). The rms error on the testing data set over the whole sunspot cycle was 0.946 MHz.

Two years of measured data from a different sunspot cycle were used to test whether the NN could successfully predict foF2 for epochs outside that for which it had been trained. Figure 6-4 shows the results for 1989 (solar maximum) and 1995 (solar minimum). The rms errors on the testing data set for 1989 and 1995 were 1.03 MHz and 0.92 MHz respectively. Of particular interest is the way in which the NN has predicted the fine structure observed between day number 200 and 250 in 1989. A detailed investigation showed that this short-term variation is definitely a response to the A16 input variable.

The IRI is the model best known for ionospheric prediction. It was used to compare the results obtained from the NN. Table 6-1 details the rms errors between the predicted and measured values for the NN and the IRI for the same data set.

(a)

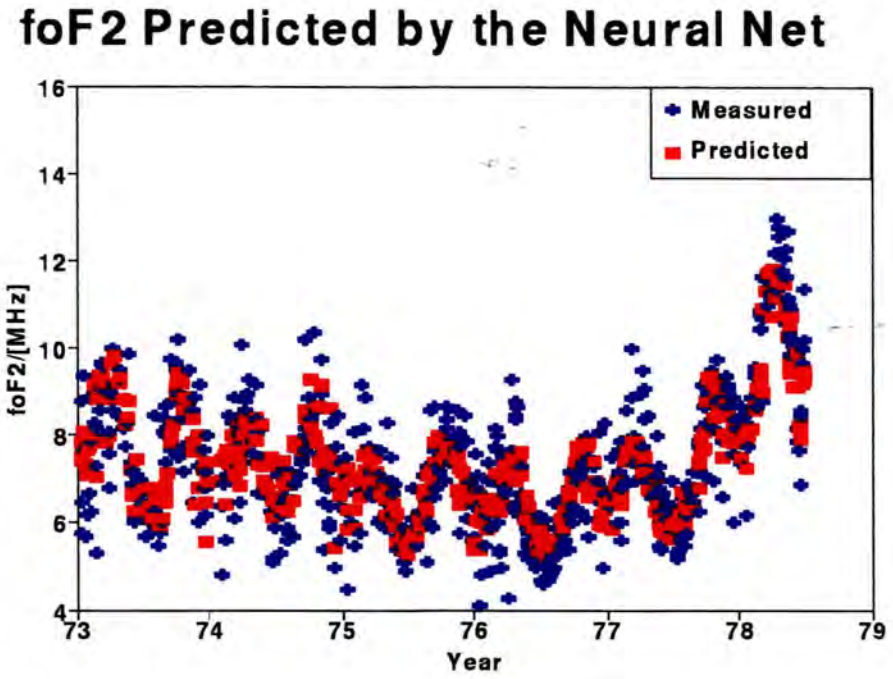

(b)

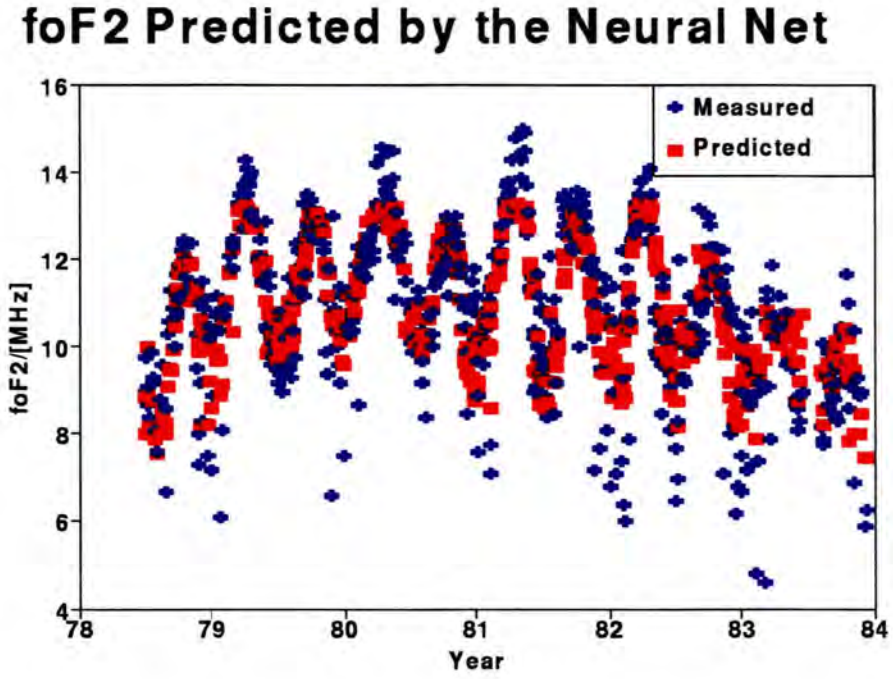

Figure 6-2: This figure shows the daily measured and predicted foF2 values of the testing data set presented chronologically, for: a) the period 1 January 1973 to 30 June 1978. The rms error was 0.85 MHz. b) the period 1 July 1978 to 31 December 1983. The rms error was 1.03 MHz.

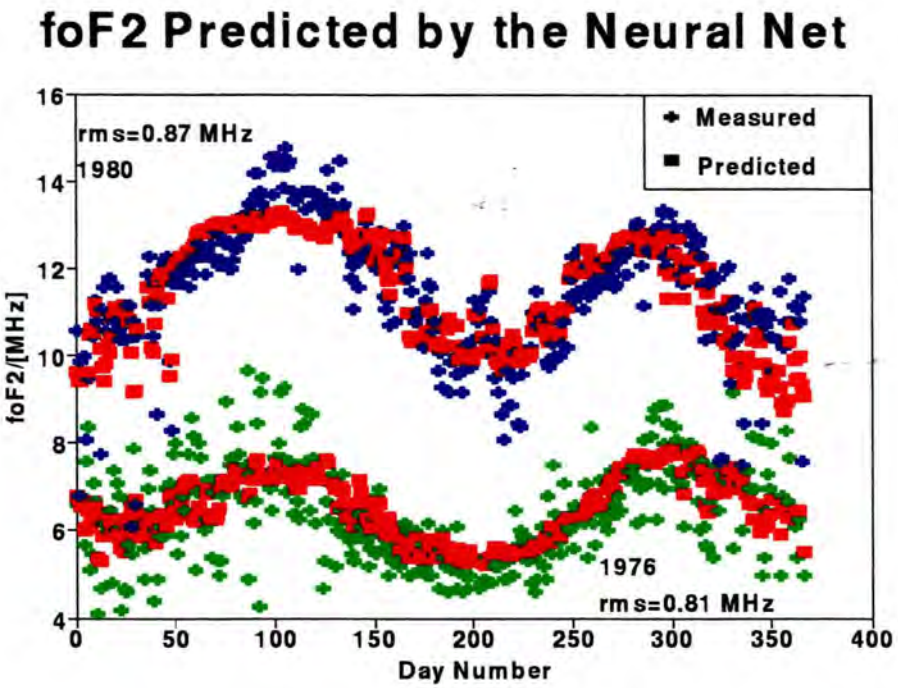

Figure 6-3: This figure shows the measured and predicted values for 1980 and 1976.

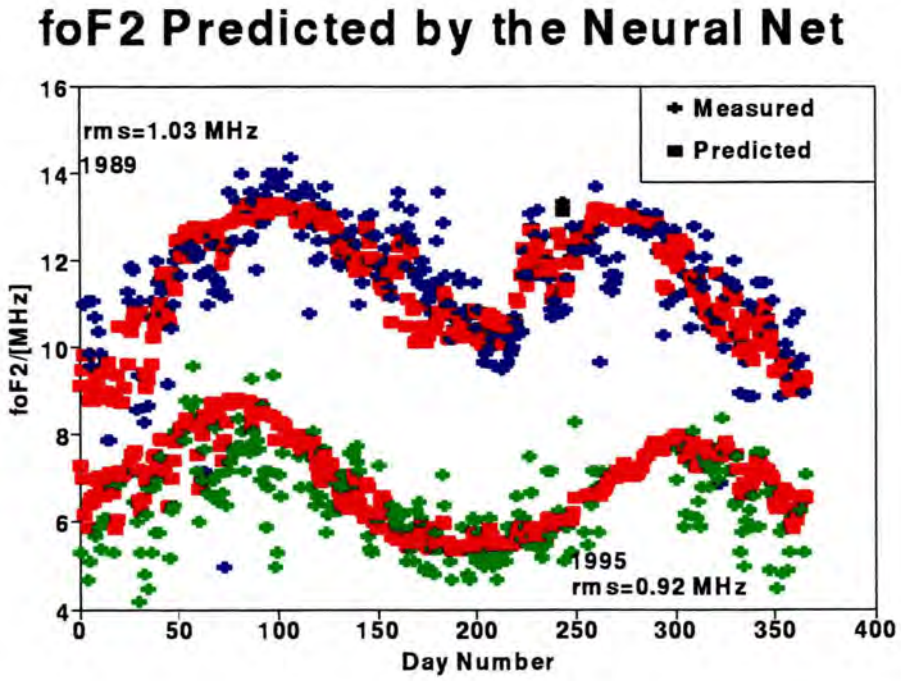

Figure 6-4: This figure shows the measured and predicted values for 1989 and 1995. The rms error values were 1.03 MHz and 0.92 MHz respectively *(after Williscroft and Poole, [1996])*.

6.5 Analysis of the Results:

The difference between the measured foF2 value and the predicted foF2 value for the original testing data set (1973 to 1983) was defined, in MHz, to be

$$DF = foF2(measured) - foF2(predicted)$$

It appears from figure 6-2 that the predicted foF2 value could be underestimating at the peak of the summer months and overestimating at the minimum of the winter months. If this statement were true then cyclic behaviour would be expected in a plot of DF as a function of time. Figure 6-5 is a graph of DF versus year for the 1973 to 1983 solar cycle. No periodicity is observed in this graph.

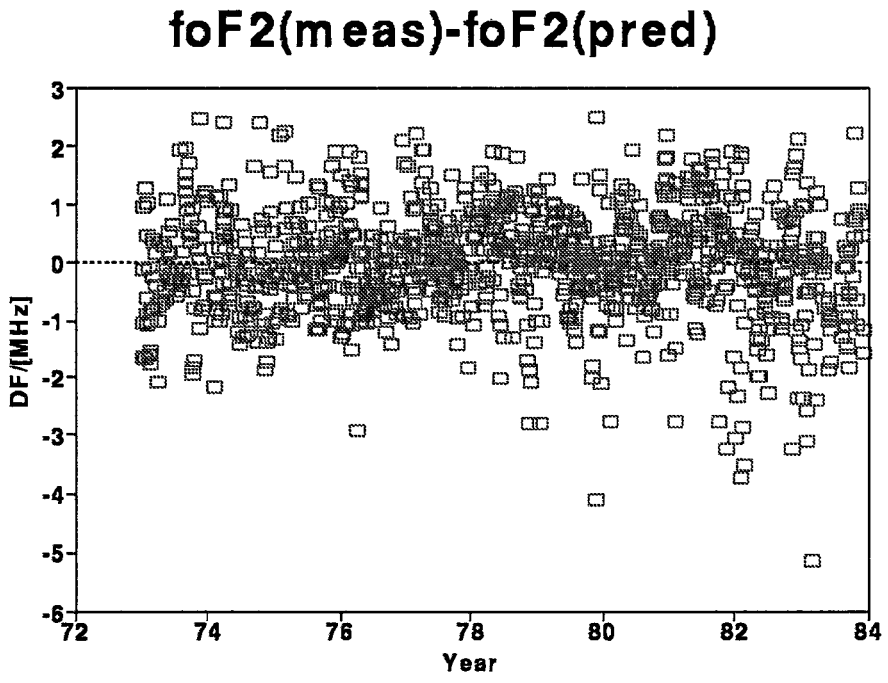

Figure 6-5: This figure shows the difference between foF2(measured) and foF2(predicted), DF, for each year of the solar cycle, 1973 to 1983.

In order to check for any residual periodicity DF was plotted against foF2(predicted). This graph is shown in figure 6-6. The correlation coefficient, $|r|$, was evaluated to test for a linear relationship between DF and foF2(predicted) which consisted of 1063 pairs of data. Statistical tables *(Rayner, [1969])* give the probability of obtaining a value of $|r|$ from random data of $25 * 10^{-3}$ or greater to be 40%, for this amount of data. Using the DF and foF2(predicted) data pairs a $|r|$ value of $22 * 10^{-3}$ was obtained. Since this value of $|r|$ could be obtained from 1063 pairs of random data 40% of the time, it is not considered to be significant.

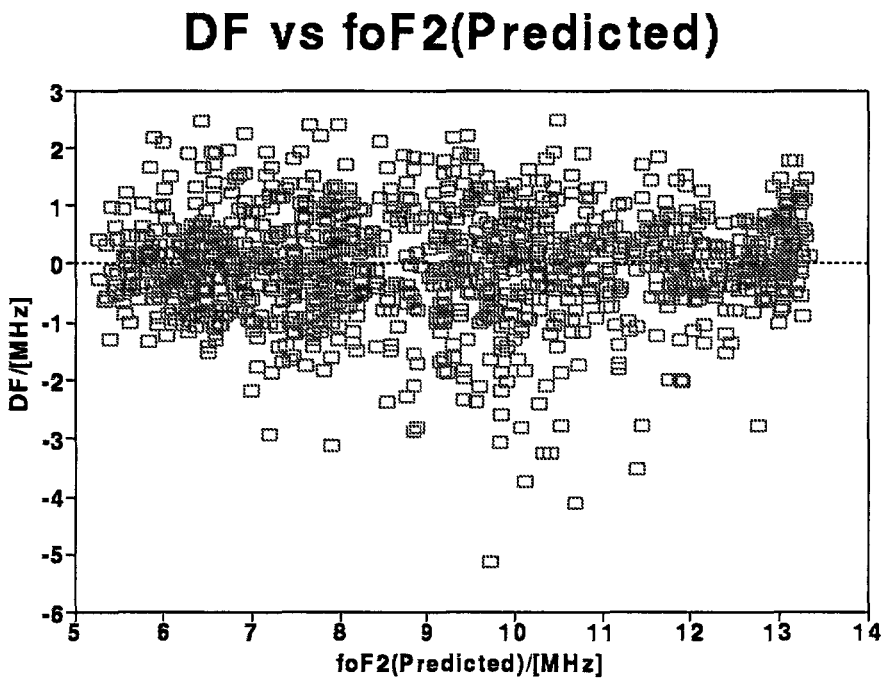

Figure 6-6: This figure shows the difference between foF2(measured) and foF2(predicted), DF, against the corresponding values of foF2(predicted) to test for any residual periodicity. The correlation coefficient, $|r|$, was $22 * 10^{-3}$.

As a further test the relationship between DF and the input parameters was examined. A linear relationship to the first order could be expected between DF and R2 or A16. However, a linear relationship is not expected between DF and the daynumber (DN) or any of its cyclic components. In view of this, DN has not been dealt with here.

Figure 6-7a, b, c, and d show graphs of R2 versus DF. The data is presented along the y-axis in order to span the entire R2 range. The graphs of A16 versus DF are presented in a similar fashion in figure 6-8a, b, and c. From these graphs it can be concluded that the difference between the measured and the predicted values is not correlated linearly with either R2 or A16, indicating that the predictive properties of these two inputs have been exhausted.

Statistical methods *(Rayner, [1969])* were used in order to perform a quantitative assessment on these data. From statistical tables, which appear in *Rayner, [1969]*, it is found that the probability of obtaining a value of $|r|$ of $3.8 * 10^{-3}$ or greater from a random set of 1063 pairs is 90%. The value of $|r|$ obtained from using the testing data set pairs of R2 and DF was $7.8 * 10^{-5}$. Since this value is much smaller than $3.8 * 10^{-3}$ it is clear that no linear correlation exists between R2 and DF. Similarly there is no linear correlation between A16 and DF as the value of $|r|$ was $1.9 * 10^{-4}$.

a)

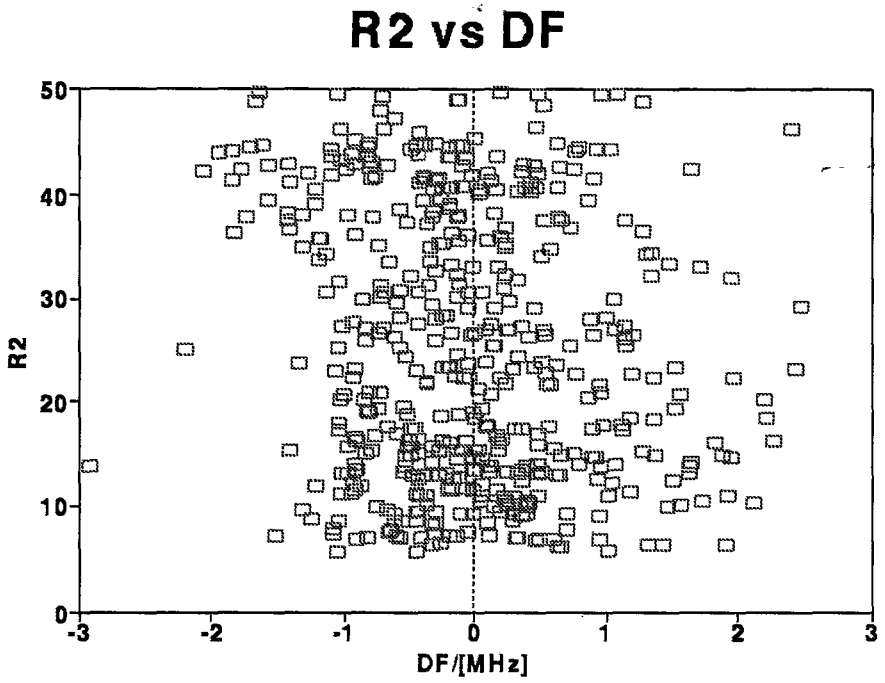
R2 vs DF
R2
DF/[MHz]
50
40
30
20
10
0
-3
-2
-1
0
1
2
3

b)

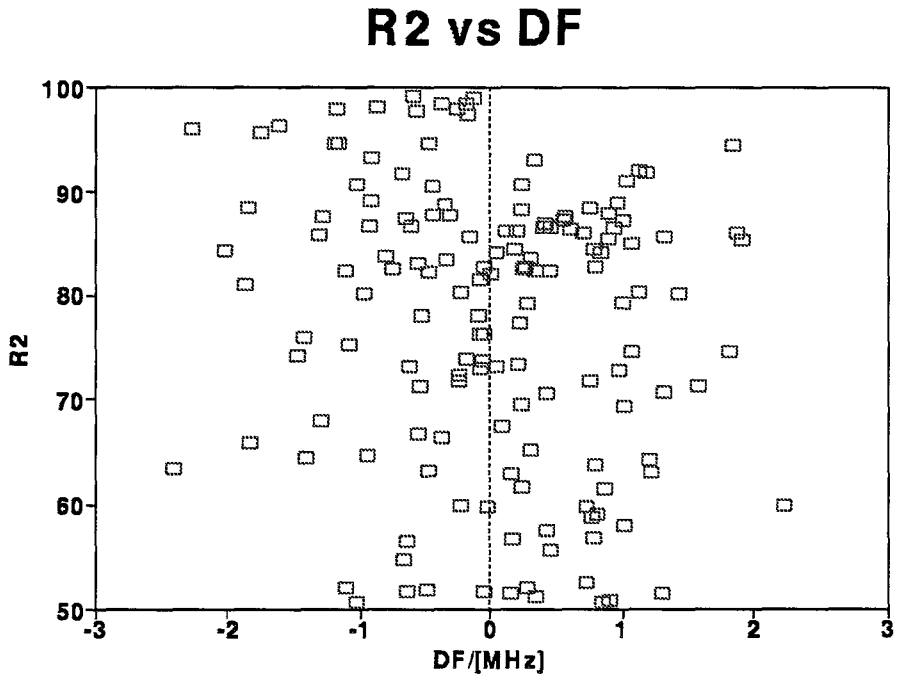
R2 vs DF
R2
DF/[MHz]
100
90
80
70
60
50
-3
-2
-1
0
1
2
3

c)

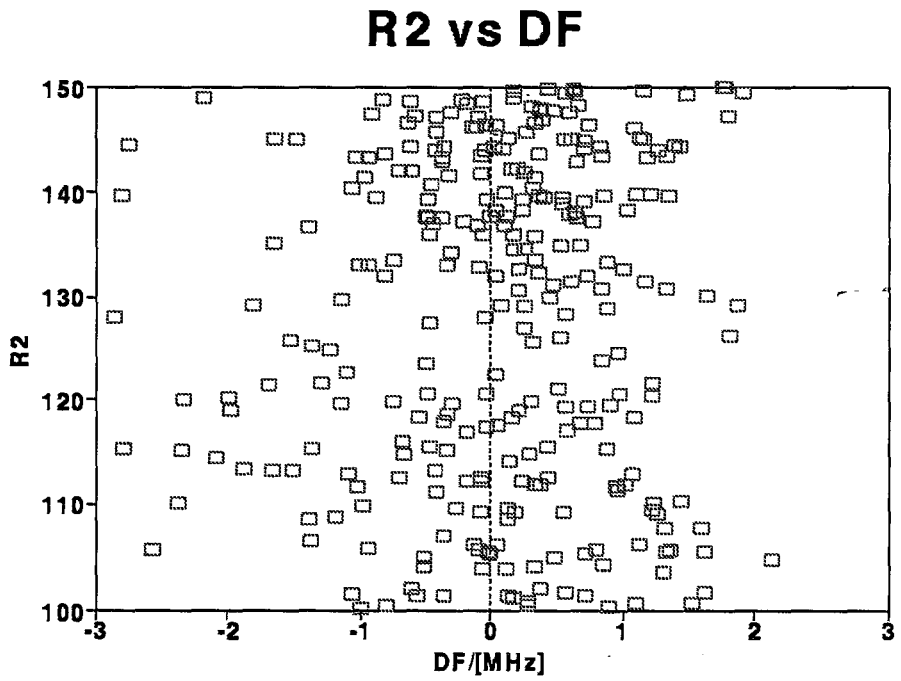

d)

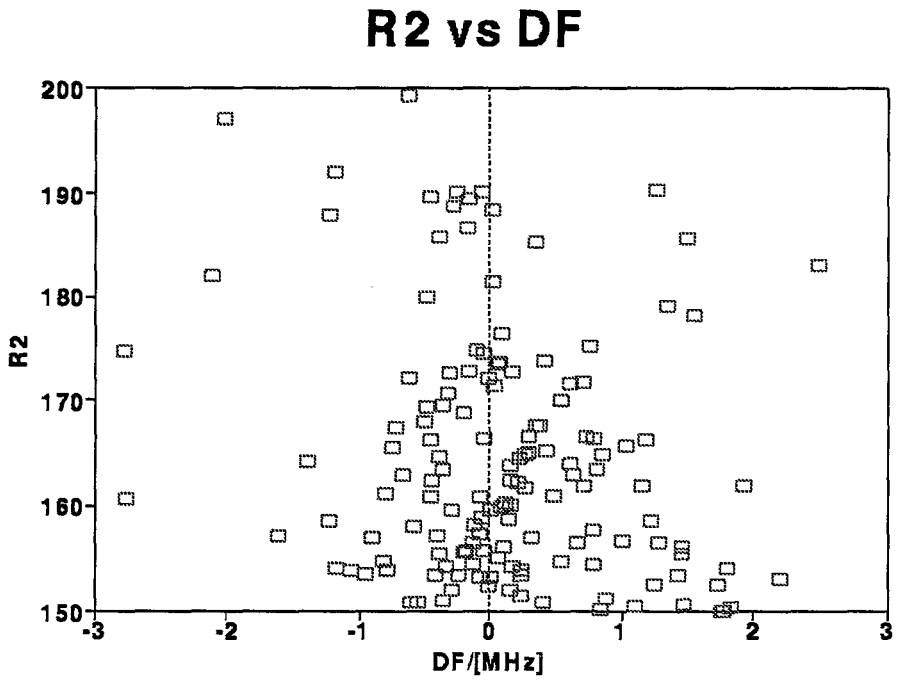

Figure 6-7: This figure shows a plot of R2 vs DF where DF is the difference between the measured and predicted foF2 values. The data is presented in 4 parts which cover the entire R2 range. The correlation coefficient, $|r|$, for all these data, was $7.8 * 10^{-5}$.

a)

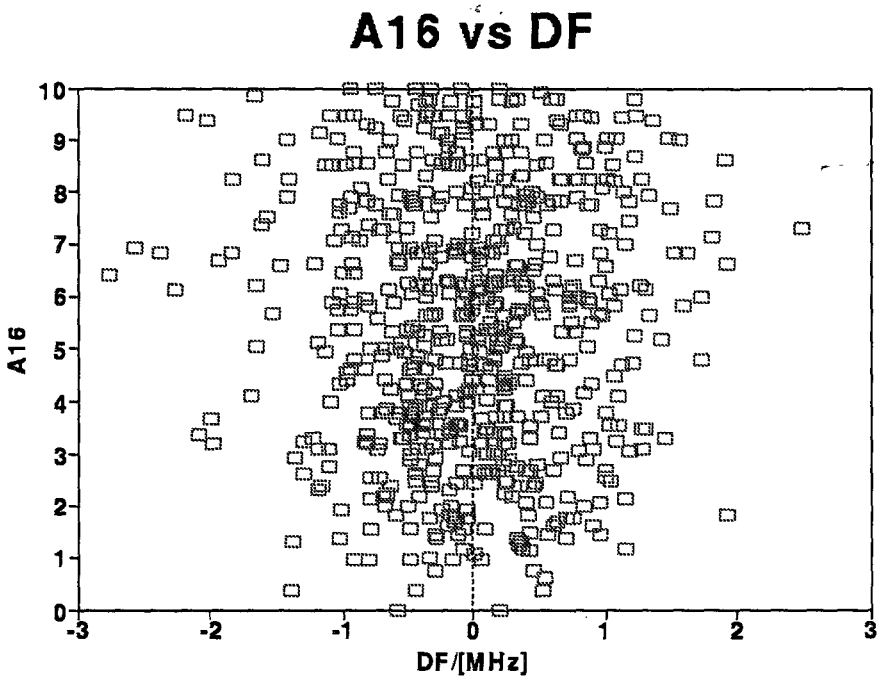
A16 vs DF
A16
DF/[MHz]
10
9
8
7
6
5
4
3
2
1
0
-3
-2
-1
0
1
2
3

b)

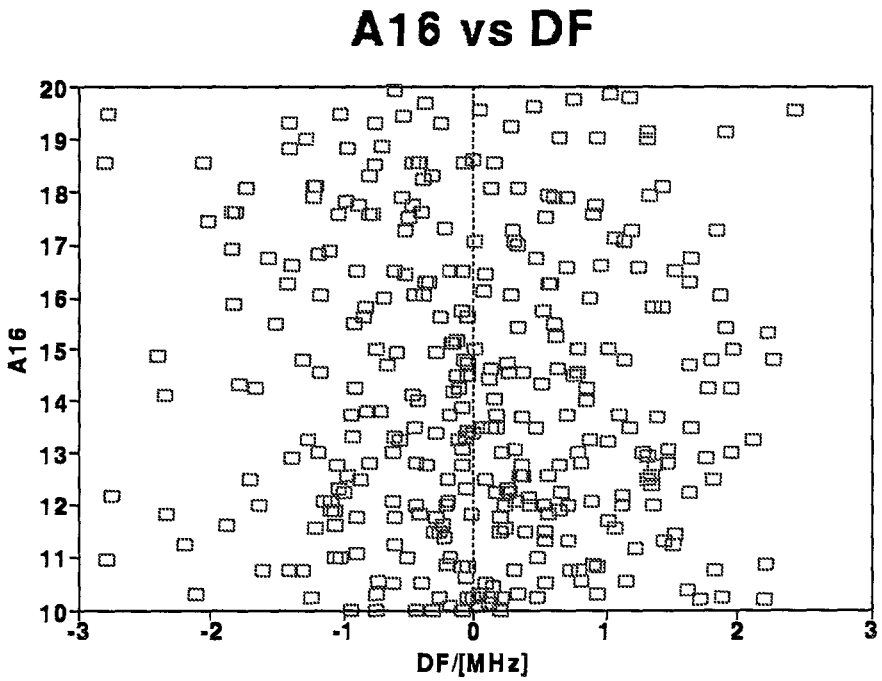
A16 vs DF
A16
DF/[MHz]
20
19
18
17
16
15
14
13
12
11
10
-3
-2
-1
0
1
2
3

c)

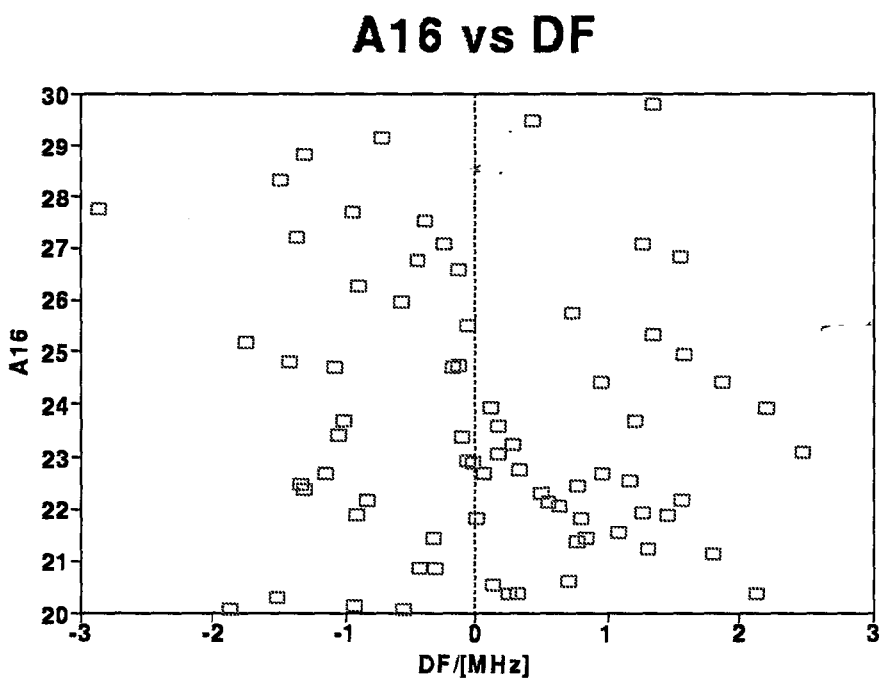

Figure 6-8: This figure shows the graphs of A16 vs DF. The data is presented in 3 parts which cover the entire A16 range. The correlation coefficient, $|r|$, was $1.9 * 10^{-4}$.

6.6 Conclusion:

The NN trained successfully to predict the 12 noon foF2 value for Grahamstown. This success was measured quantitatively in terms of the rms error between the measured and predicted values. Comparison with the IRI shows a significant improvement in the rms error, as shown in table 6-1.

The analysis, both quantitative and qualitative, of the difference between the measured and predicted foF2 values showed that the NN has used all the information available to it. Another predictor of foF2 may be required in order to eliminate this residual difference. Further research is to be undertaken in this area.

The research presented in this chapter was the subject of a poster presentation at the XXVth General Assembly of the International Union of Radio Science in Lille, France.

Chapter 7

APPLYING THE NEURAL NET

7.1 Introduction

The previous chapter showed how a neural net (NN) was trained to predict foF2 given two components of day number (DN), sunspot number (SSN) and magnetic index (MI). This NN now contains all the information inherent in these parameters. This chapter reveals how the relationship between foF2 and any one of the three input variables can be found using the NN. This is described in the first section of this chapter.

It is shown that the relationship between foF2 and MI over an entire year is very non-linear, and depends on season. In the second section of this chapter the NN is used very simply to find the variation in noon foF2 at times of high and low magnetic activity, for different times in the sunspot cycle as a function of day number. The results are compared with those of *Fuller-Rowell et al, [1996]*, who used a number of complicated numerical simulations to investigate the response of the ionosphere to geomagnetic storms.

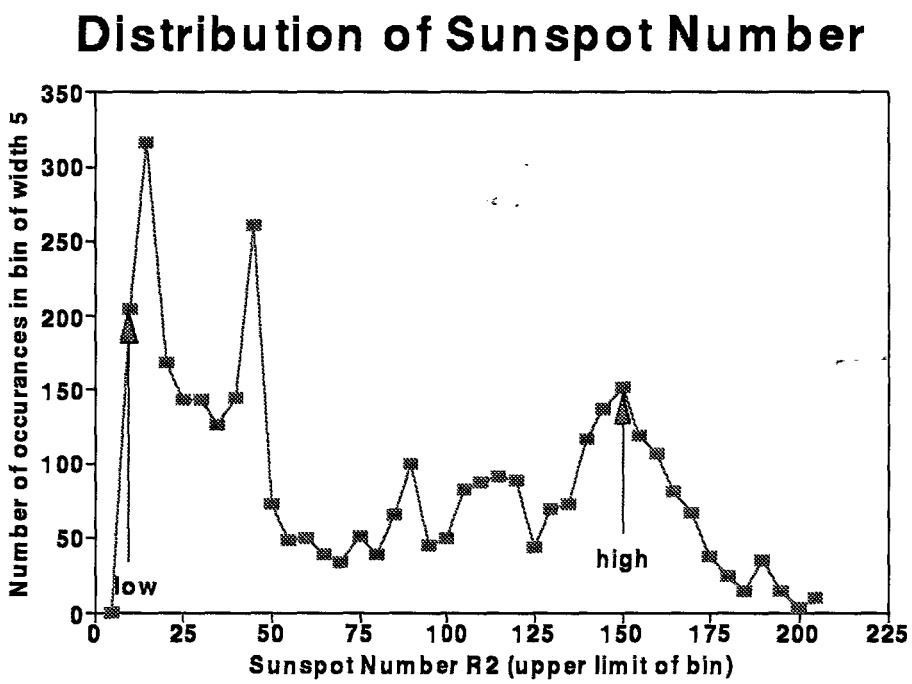

Figure 7-1: The distribution of the R2 values, calculated for the period 1973 to 1983, which was used to choose typical values of "low" and "high" solar activity.

7.2 Input Analysis

In order to investigate the relationship between foF2 and DN, SSN or MI, three different sets of test data were set up as follows:

(i) DN over the range 1 to 365, fixed SSN and MI,

(ii) SSN over the range 6 to 150, fixed DN and MI,

(iii) MI over the range 0 to 25, fixed DN and SSN.

HIGH & LOW VALUES		
Input	High	Low
DN	180 (winter)	1 (summer)
SSN	150 (high)	10 (low)
MI	25 (disturbed)	5 (quiet)

Table 7-1: The chosen high and low values for each input parameter.

For each of these cases the fixed parameters were set at typical high and low values. The values of DN chosen were 1 as being typical for the summer months and 180 for the winter months. For the SSN, values of 10 and 150 were chosen as typical indicators of times of low and high solar activity. These values were selected from the distribution of R2 as shown in figure 7-1. A day where the MI value is low is usually referred to as a magnetically "quiet" day and a day where the MI value is high is referred to as a magnetically "disturbed" day. The quiet and disturbed day values were chosen from the distribution shown in figure 7-2 to be 5 and 25 respectively. The values for both the SSN and the MI inputs were chosen so that about 70% of the data lay between the low and high values selected and 15% at each end. Table 7-1 summarises these high and low values.

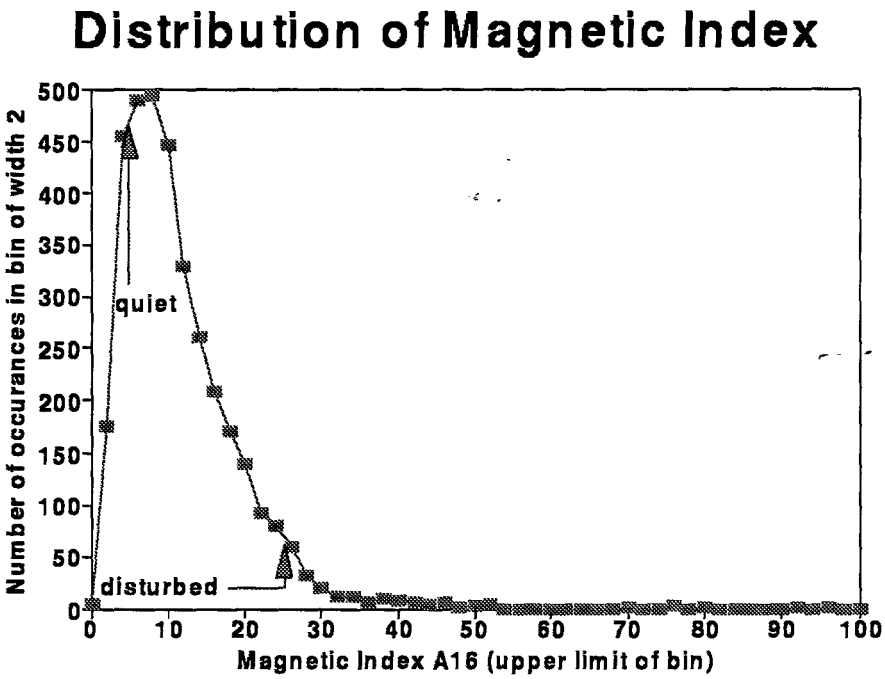

Figure 7-2: The distribution of A16, for the period 1973 to 1983, which was used to choose typical values to represent magnetically quiet (low) and disturbed (high) days.

7.2.1 Day Number

A set of data was constructed where the DN input varied from 1 to 365 and the SSN and MI inputs were fixed. The cosine and sine components of the DN value were used as inputs to the NN as described in chapter 5. Four subsets of the data were created with the four combinations of high and low SSN and MI. The NN predicted the 12 noon foF2 value for each subset of inputs. Figure 7-3 shows the four plots of foF2 versus day number. From this graph it is observed that at times of high sunspot number foF2 increases with an increase in MI during the winter months but decreases with an increase in MI during the summer months. The same observation can be made at times of low SSN, only the effect is less pronounced. This is an important result which came about easily with the use of a NN. *Fuller-Rowell et al., [1996]* came to the same conclusion using numerical simulations. This is discussed in more detail later in this chapter.

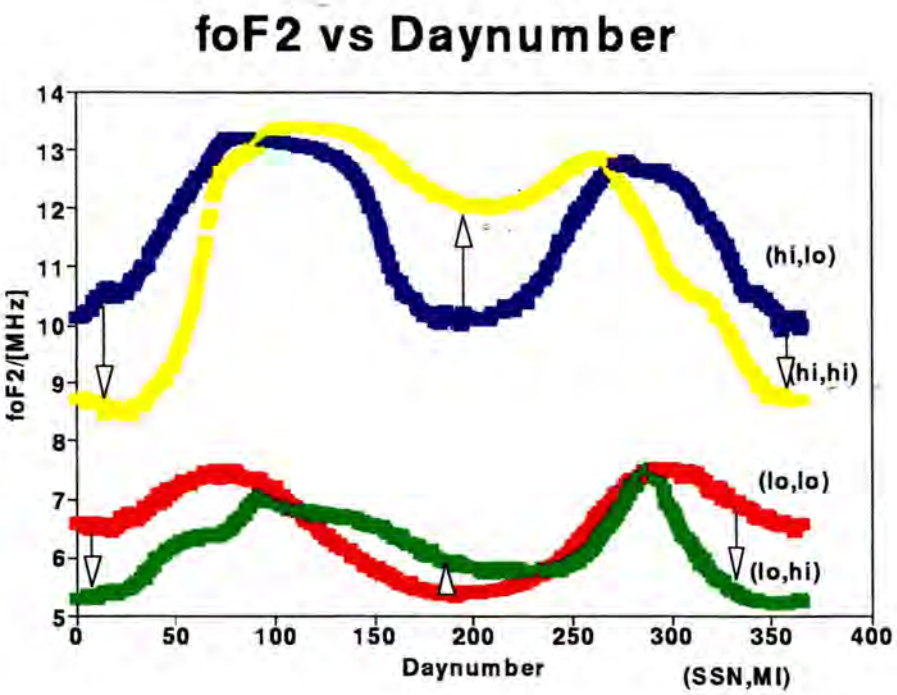

Figure 7-3: A graph of predicted values of noon foF2 during quiet and disturbed periods of magnetic activity, for different levels of solar activity. The arrows indicate the direction of increase or decrease with change from quiet to disturbed.

7.2.2 Sunspot Number

For the second case, the SSN was allowed to vary from 6 to 150 while the DN and MI inputs were fixed. Four subsets of this data were constructed by making use of all the possible combinations of the inputs. The NN predicted the noon value of foF2 for each case. Figure 7-4 shows the graphs of foF2 versus SSN during winter and summer at magnetically quiet and disturbed times. From these graphs it appears that foF2 experiences a quasi-linear increase with SSN for all values of season and MI. The arrows indicate the direction of increase or decrease with change from quiet to disturbed, and once again illustrates the reversed behaviour for the different seasons.

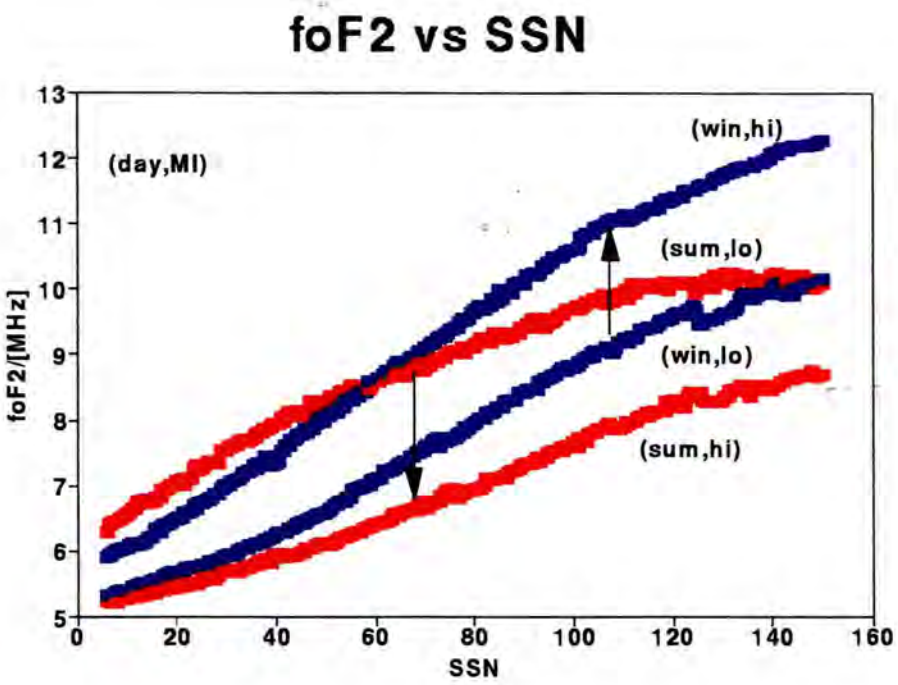

Figure 7-4: This graph represents the seasonal change in foF2 as the SSN increases for quiet and disturbed periods of magnetic activity.

7.2.3 Magnetic Index

Finally, the magnetic index was allowed to vary from 0 to 25 while the DN and the SSN were kept constant. The NN predicted the noon foF2 value at times of high and low SSN during summer and winter. Figure 7-5 shows the graphs of foF2 versus MI. These graphs show a quasi-linear change in foF2 with MI, however the slope of foF2 versus MI is positive in the winter and negative in the summer.

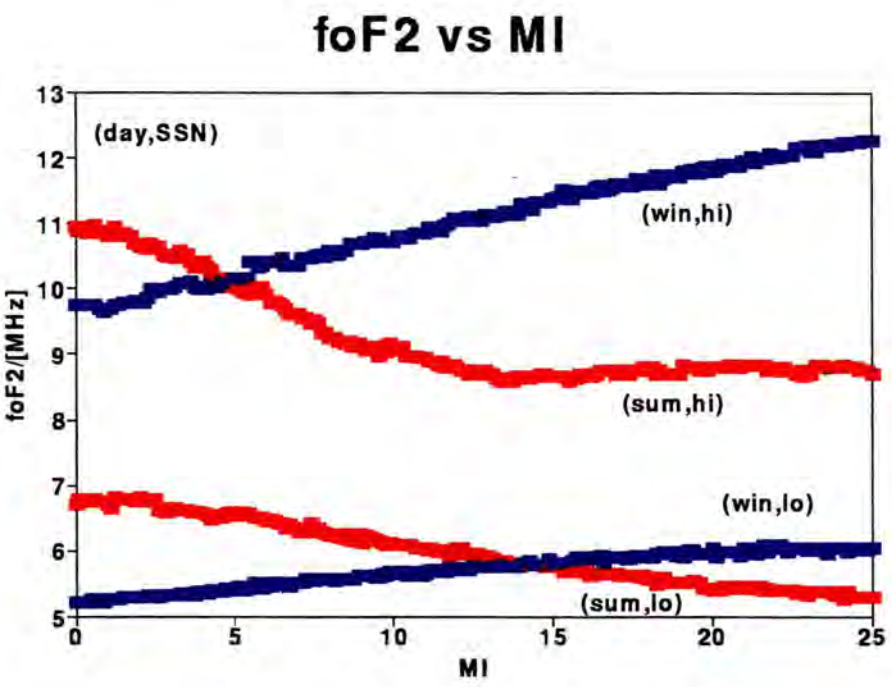

Figure 7-5: This graph shows how foF2 is influenced by magnetic activity during summer and winter at different times of the solar cycle.

7.3 Neural Net Response to Magnetic Activity

After training the NN can be used as a tool for investigating the change in foF2 that results from different input parameters. *Fuller-Rowell et al., [1996]* investigated the seasonal response of the mid-latitude ionosphere to geomagnetic storms. In this section the NN is used to provide support for this research. The trained NN was used to find values of foF2 at magnetically quiet and disturbed times, for different times in the sunspot cycle, as a function of day number. A graph of foF2 versus day number appears earlier in this chapter in figure 7-3.

A difference is defined as

$$DfoF2/[MHz] = foF2(disturbed) - foF2(quiet)$$

where foF2(disturbed) and foF2(quiet) are the predicted values of foF2 at times of disturbed and quiet magnetic activity respectively. Figure 7-6 is a plot of DfoF2 in MHz against day number for high and low times of the solar cycle. The difference is negative in the summer months and positive in the winter months. This observation is consistent with the findings of *Fuller-Rowell et al., [1996].* The difference appears to be less at times of low solar activity than at times of high solar activity.

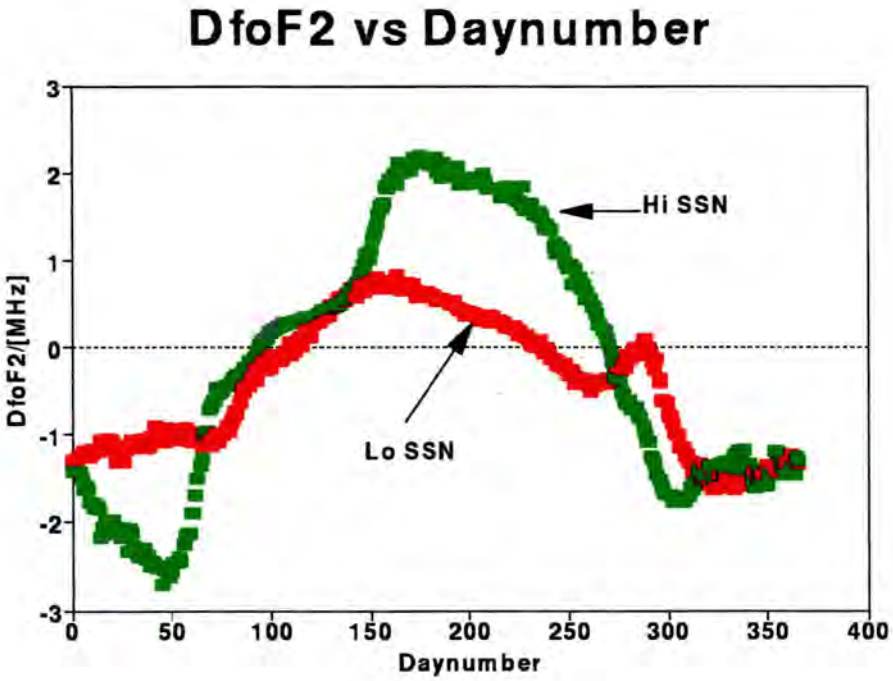

Figure 7-6: This graph plots the difference, DfoF2, as a function of day number for low and high sunspot number.

7.4 Conclusion

NNs can be applied to geophysical problems. A NN that had been trained with real data was used to investigate the influence of day number, sunspot number and magnetic activity on the noon value of foF2.

An important finding of the research presented in this chapter is the NNs response to magnetic activity. This response changes as the level of magnetic activity goes from quiet to disturbed and the direction of this change depends upon season. This demonstrates a highly non-linear response of foF2 to MI. In the same way, the NNs response to the variable SSN was also found to be non-linear and dependent on season. Regression techniques could not be used to show this behaviour which illustrates the extreme capabilities of NNs. As well as being used for predictive modelling, NNs can determine relationships between variables with comparative ease.

Chapter 8

CONCLUSION

The aim of the research laid out in this thesis was to find a temporal model for predicting the maximum electron density (foF2) of the ionosphere. The Hermann Ohlthaver Institute for Aeronomy (HOIA), based in Grahamstown, has been operating a vertical incidence ionosonde for more than 20 years. Consequently, there is a large database of ionospheric information available for such research. The possibility of a prediction model for foF2 was investigated by using a subset of this database. This subset consisted of the 12 noon foF2 values over Grahamstown for the years 1973 to 1983 inclusive.

The IRI and SKYCOM are two ionospheric prediction packages that exist already. Both of these were found to be lacking when predicting foF2 over Grahamstown at 12 noon. Chapter 2 discusses each of these models and their performance.

The first step towards finding an improved model of foF2 over Grahamstown was to attempt linear regression on the available data. Chapter 3 showed that foF2 does depend on the day number, the sunspot number and the level of magnetic activity and therefore a multivariable regression would be required in order to find a predictive model equation. The optimum variables needed in the final equation would have to be guessed. This would be an extremely complicated modelling equation with many terms.

A new method for modelling parameters is that of neural networks (NNs). A NN can be trained by presenting to its input any number of multidimensional vectors that correspond to a known output parameter. Chapter 4 discusses the theory behind the NNs used in this thesis.

NNs were also used to determine the best predictors of foF2. Chapter 5 showed that the optimum predictors of the 12 noon foF2 value were the 2-month running mean sunspot number (R2) and a 2-day averaged magnetic A-index value (A16). An important finding of this research is the response of foF2 to changes in the level of magnetic activity. A highly non-linear response of foF2 to magnetic index was demonstrated in chapter 7. Regression techniques were unable to show this response.

The results from training the NN are presented in chapter 6. One solar cycle of 12 noon data, 1973 to 1983, were used to train the NN. The architecture of the NN used here is shown in figure 4-5. The ability of the NN to predict was measured in terms of the rms error between the measured and predicted foF2 values. There was a significant improvement of the NN in the rms error compared with that obtained from the IRI. An analysis of the difference between the measured and predicted values showed that the NN had used all the information available to it. It is possible that another predictor of foF2 is required in order to reduce this difference. This is an area where further research could be done.

Chapter 3 dealt with an attempt to model foF2 using linear regression. The data set used consisted of the 12 noon mean foF2 values for July of each year from 1973 to 1983 inclusive. Using the NN the rms error between the measured and predicted mean July foF2 values was found to be 0.29 MHz. This value is comparable with the rms error of 0.35 MHz found by the IRI for the same data set. However, neither of these values can be compared with the rms errors obtained from using the regression equations 3-1, 3-2 and 3-3, quoted in table 3-1. The reason is that the linear regression technique applied in chapter 3 made no attempt to ensure a general result. By adding appropriate additional terms to the regression equations, the rms

error between the measured and predicted values can be made arbitrarily small, which means that the data set has been too specifically fitted. NNs give the best net that will simultaneously allow generalisation. In other words, a NN can be used on a different data set of the same type whereas the regression equation is too data set specific to be applied to another data set. Furthermore, since the regression technique was only applied to 1 month, July, new regression coefficients would have to be found for the other months.

The subject of this thesis has been presented in various stages of the research at four different local conferences and one international conference. At all of these meetings the research papers received favourable review. A paper entitled "Neural Networks, foF2, Sunspot Number and Magnetic Activity" has been accepted for publication in Geophysical Research Letters. The contents of chapters 5 and 6 form the subject of this paper.

NNs can provide a way to combine large data sets into a model to predict foF2. The data set used here could be expanded to include all hours of the day for Grahamstown, and then presented to the net for re-training. Future plans for ionospheric research in South Africa include two more ionospheric stations at the extreme boundaries of the country. Both of these stations plus the Grahamstown station will contribute over time towards a complete database of ionospheric measurements over South Africa. This database will contain information that could be used by a NN to demonstrate the behaviour of the ionosphere over the entire country. The data set could then be further expanded to include latitude and longitude information and therefore provide a spatially, as well as temporally predictive model for South Africa. A natural progression from here would be to use the NN to produce a global predictive model for foF2, covering all hours of the day and all locations. This thesis is the first step towards the attainment of that goal.

Chapter 9

REFERENCES

- Bilitza D., *International Reference Ionosphere,* National Space Science Data Center, 1990.
- Borland International, *QuattroPro version 3.0*, 1991.
- Fausett L., *Fundamentals of Neural Networks*, Prentice-Hall International Inc., 1994.
- Fuller-Rowell T.J., M.V.Codrescu, H. Rishbeth, R.J. Moffett, and S. Quegan, On the seasonal response of the thermosphere and ionosphere to geomagnetic storms, *Geophys. Res. Let., Vol 101*, pp. 2343-2353, 1996.
- Haykin S., *Neural Networks, A Comprehensive Foundation*, Mcmillan Publishing Company, Inc., 1994.
- Matsushita S., and W.H. Campbell (Eds.), *Physics of Geomagnetic Phenomena Vol 1,* 67-98, Academic Press, New York, 1967.
- McNamara L.F., *The Ionosphere: Communications, Surveillance, and Direction Finding,* Krieger Publishing Company, 1991.

- Mosteller F. and J.W. Tukey, *Data analysis and Regression*, Addison-Wesley Publishing Company, 1977.

- NeuralWare release A11, *NeuralWorks Predict (TM)*, U.S.A., 1995.

- Rayner A.A., *A first course in biometry for agriculture students*, 334 ff., University of Natal Press, Pietermaritzburg, 1969.

- Rush C.M., M.PoKempner, D.N.Anderson, F.G.Stewart, and J.Perry, Improving ionospheric maps using theoretically derived values of foF2, *Radio Science, 18,* 95-107, 1983.

- Williscroft L.A., and A.W.V.Poole, Towards a standard reference ionosphere for the South African region, *AP/MTTS 1995 Proceedings*, 180- 185, 1995.

- Williscroft L.A., and A.W.V. Poole, Neural Networks, foF2, sunspot number and magnetic activity, *Geophys. Res. Let., In press,* 1996.